THE PERFORMANCE OF SILICA-TITANIA COMPOSITES IN A PACKED-BED REACTOR FOR PHOTOCATALYTIC DEGRADATION OF GRAY WATER

By

CHRISTINA YVETTE LUDWIG

A THESIS PRESENTED TO THE GRADUATE SCHOOL
OF THE UNIVERSITY OF FLORIDA IN PARTIAL FULFILLMENT
OF THE REQUIREMENTS FOR THE DEGREE OF
MASTER OF ENGINEERING

UNIVERSITY OF FLORIDA

2004

ACKNOWLEDGMENTS

I would like to thank my advisor, Dr. David Mazyck, for the opportunity to perform this research and for his guidance. It has been a challenging and rewarding experience to learn from him. I would also like to thank the other members of my committee, Dr. Paul Chadik, Dr. Kevin Powers, and Dr. Chang-Yu Wu, for their constant supply of knowledge and suggestions throughout the duration of this research.

I am grateful for the opportunity to work as part of an excellent research group. I thank Ameena Khan, Matt Tennant, Thomas Chestnutt, Jack Drwiega, Jennifer Hobbs, Jennifer Stokke, Morgana Bach, and Danielle Londeree for their ideas and suggestions as well as their general support and advice. Each group member contributed to this research as well as my education.

I must also thank my family for all their love and support. Special thanks go to my husband, Matthew, for his constant encouragement and support throughout all of my education.

TABLE OF CONTENTS

page

LIST OF TABLES

LIST OF FIGURES

Abstract of Thesis Presented to the Graduate School
of the University of Florida in Partial Fulfillment of the
Requirements for the Degree of Master of Engineering

THE PERFORMANCE OF SILICA-TITANIA COMPOSITES IN A PACKED-BED REACTOR FOR PHOTOCATALYTIC DEGRADATION OF GRAY WATER

By

Christina Yvette Ludwig

August 2004

Chair: David Mazyck
Major Department: Environmental Engineering Sciences

Photocatalysis is used to mineralize organic water pollutants, providing water treatment without a waste stream. This water treatment method allows for a compact reactor design that is applicable in future NASA missions that will require water recovery. The objective of this research was to optimize a photocatalytic reactor that will reduce the total organic carbon (TOC) concentration of a gray water influent to meet NASA's drinking water quality standards. The system utilizes a reactor packed with titanium dioxide (TiO_2) supported by silica gel (SiO_2) and was optimized with respect to empty bed contact time (EBCT), pore size of the SiO_2-TiO_2 composite, and TiO_2 loading of the SiO_2-TiO_2 composite. The addition of activated carbon to the SiO_2-TiO_2 composite was also investigated.

An optimum EBCT of seven minutes was found based on the fastest destruction rate to reach below the 500 ppb TOC maximum limit established by NASA. Also based on destruction rate, a SiO_2-TiO_2 composite having a 12% TiO_2 loading (weight/volume

basis) and 118 angstrom pore size was shown to have the best performance. Activated carbon was found to improve the overall performance of the system through its increase to the composite's adsorption capabilities. Greater adsorption capabilities can allow for lower energy requirements, enabling the UV light to be turned off during a period of contaminant adsorption and turned on for mineralization of the contaminants already surrounding the photocatalyst.

Adsorption capabilities of the support can lead to more efficient, complete destruction of the contaminants by surrounding the photocatalyst with a high concentration of contaminants; therefore, it was predicted that increasing the ability of the photocatalyst composite to adsorb the organic contaminants would increase the rate of photocatalytic destruction. Adsorption was shown to be an important system parameter, but increasing adsorption did not always lead to a better destruction rate due to the contribution of other parameters controlling the system, such as UV light exposure and hydraulic flow through the reactor.

CHAPTER 1
INTRODUCTION

Contamination of our water, air and soil by various agricultural and industrial processes has traditionally been controlled through ultrafiltration, extraction, air stripping, carbon adsorption, incineration, and oxidation via ozonation or via hydrogen peroxide (Serpone, 1995). Problems with the successful and efficient removal of toxic pollutants from our environment have led to the search for more advanced methods (Hoffmann et al., 1995). Groundwater contamination is expected to be a primary source of human contact with a majority of the toxic pollutants in our environment, many of which are organic compounds, such as solvents, pesticides, chlorophenols, and volatile organics (Hoffman et al., 1995). Photocatalysis offers an advanced technology for the removal of toxic organics from our water. Many of the previously mentioned technologies simply transfer the pollutant out of the water, requiring additional treatment and/or disposal of the compound. In photocatalysis, the organic contaminants are oxidized, ultimately to carbon dioxide and water, leaving no waste to dispose. Utilizing UV irradiation, photocatalysis has the added advantage of being able to simultaneously disinfect and destroy organics (Serpone, 1995). Because of its promise as a more advanced environmental technology, photocatalysis is being developed for the destruction of toxic organic compounds in water. Given its ability to eliminate organic compounds in one process, this technology has a variety of applications.

Its potential to be a compact, low maintenance system makes it particularly useful for small-scale water recovery. Water recovery is a vital component of NASA space

missions. The reclamation of water from gray sources, which include shower waste, hand wash waste, oral hygiene waste, urine, urine flush waste, and spacecraft humidity condensate, enables long-term presence in space without the penalty of transporting large masses of clean water to the crew members. It is also a necessity for missions involving long flight distances, such as a mission to Mars. It is important that the water recovery system be compact and reliable with as little energy requirements as possible, allowing crew members to direct time and resources toward scientific investigations. A photocatalytic system that meets NASA's water recovery system requirements is being developed to be used as a post processor for the destruction of organic compounds that may not be removed in preceding water subsystems. These subsystems may include biological reactors, ion exchange, and reverse osmosis. The objective of the post processor is to ensure that the total organic carbon (TOC) concentration remains below the maximum limit required by NASA water quality standards, which is 500 ppb (Lange and Lin, 1998). The post-processor must also be able to treat the wastewater at a rate of 11.5 L/person/day, which is the quantity of wastewater produced by each person per day (Campbell et al., 2003).

A system that destroys organic contaminants would also be applicable in a home water treatment system. Some homeowners, particularly those with well water as their water supply source, choose to use additional treatment processes, such as an activated carbon filter, before consumption. Depending on the water quality, it is suggested that 10 to 20 L/day of water for drinking or cooking could be processed using a 15 W to 40 W photocatalytic unit at a cost comparable to other treatment processes (Matthews, 1993).

The ability of photocatalysis to mineralize organic compounds has already been proven (Matthews, 1987). More efficient, complete destruction of organic compounds in water can be achieved through the use of an adsorbent as a support for the photocatalyst. Because silica is transparent, it does not interfere with the absorbance of energy on the titania surface but does provide a means of immobilizing the titania to avoid the issue of separating it from the water after treatment. The porous structure of silica also allows for the adsorption of contaminants, providing a pathway to the photocatalyst. Adsorption capabilities can also allow for lower energy requirements, enabling the UV lamp to be turned off during a period of contaminant adsorption and turned on for mineralization of the contaminants already surrounding the photocatalyst.

The overall objective of this research is to optimize a photocatalytic reactor system that will reduce the TOC concentration of a gray water influent to meet NASA's drinking water quality standards. The system will utilize a reactor packed with titanium dioxide (TiO_2) supported by silica gel (SiO_2) and will be optimized with respect to empty bed contact time (EBCT), pore size of the SiO_2-TiO_2 composite, and TiO_2 loading of the SiO_2-TiO_2 composite. The addition of activated carbon to the SiO_2-TiO_2 composite will also be investigated. Increasing the ability of the photocatalyst composite to adsorb the organic contaminants is expected to increase the rate of photocatalytic destruction; therefore, it is predicted that the composite characteristics resulting in the highest adsorption will also provide the best photocatalytic degradation of the contaminants. Because activated carbon is known as an adsorbent of organic compounds, it is hypothesized that the addition of activated carbon to the SiO_2-TiO_2 composite will increase the photocatalytic destruction rate of the system. Because activated carbon is

opaque, it may prevent some of the UV light from reaching the photocatalyst. There may be a need to balance the adsorption and the opacity, resulting in an optimum activated carbon loading.

CHAPTER 2
LITERATURE REVIEW

Photocatalysis

Heterogeneous photocatalysis involves more than one phase. In this discussion, the media involved in the reaction are a solid phase catalyst and a liquid solution containing the organic contaminants. The photocatalytic process begins with the excitation of an electron (Eq. 1).

$$TiO_2 + h\nu \rightarrow e^- + h^+ \qquad \text{(Eq. 1)}$$

When light of the appropriate wavelength is absorbed by the catalyst (e.g., TiO_2), an electron (*e*-) is transferred from the valence band to the conduction band, leaving a positively charged hole behind (*h*+). The wavelength of light necessary to provide the energy to move the electron into the conduction band varies with the specific photocatalyst; for titanium dioxide (TiO_2), UV light of less than 388 nm is required. The electron can then recombine with the electron hole, or the hole can react with other species. Oxygen plays an important role as an electron acceptor, thus preventing the electrons from recombining and keeping the electron holes open for reaction. Water and hydroxide ions react with the electron holes to form hydroxyl radicals, proven the primary oxidant in the photocatalytic oxidation of organics (Turchi and Ollis, 1990). Repeated hydroxyl radical attack can eventually lead to complete oxidation of the contaminant.

Titanium Dioxide

Titanium dioxide is the photocatalyst most often used due to its low cost and better activation over other photoactive metal oxides. It has also shown stability in that the TiO_2 itself does not change over time, unlike other photocatalysts. Zinc oxide has shown good photocatalytic abilities, but has been found to be unstable due to photodecomposition (Peral et al., 1988).

TiO_2 can be synthesized in different crystalline forms. The two most applicable structures are anatase and rutile. Both consist of titanium atoms surrounded by six oxygen atoms in different octahedron formations (Figure 1).

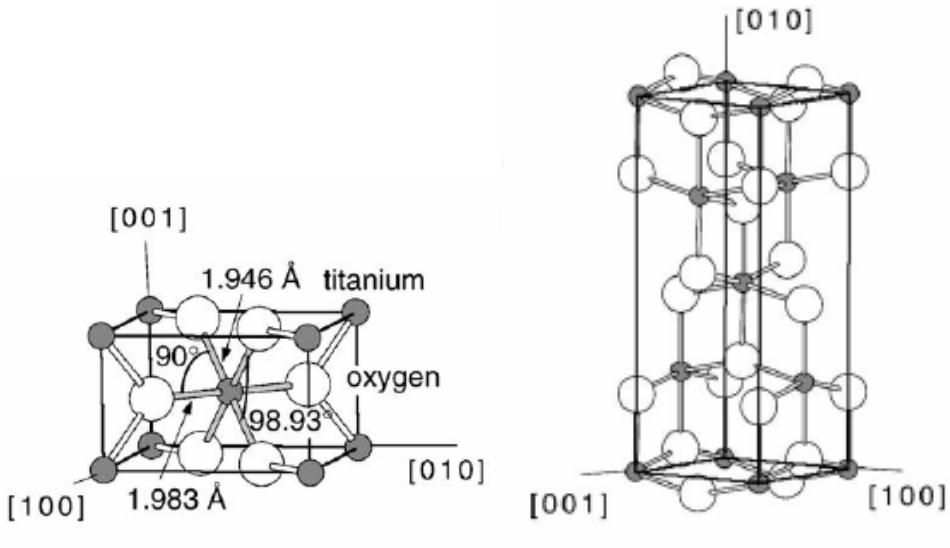

Figure 1. Illustrations of TiO_2 crystalline structures: rutile (left) and anatase (right).

The anatase structure has been found to be more photocatalytically active (Ohtani and Nishimoto, 1993; Tanaka et al., 1993). Degussa P-25 is a commercially available TiO_2 with a structure that is 70% anatase and 30% rutile. This particular TiO_2 is

commonly used as it has repeatedly demonstrated successful photocatalytic degradation of organics.

Kinetics

Langmuir-Hinshelwood (LH) kinetics has been shown to successfully describe the photocatalytic degradation of organic contaminants (Al-Ekabi and Serpone, 1988; Turchi and Ollis, 1989). The LH model assumes the reactions take place at the surface of the catalyst, and the reaction rate is proportional to the fraction of the surface covered by the reactant.

$$r = -\frac{dC}{dt} = k\theta = \frac{kKC}{1+KC} \qquad \text{(Eq. 2)}$$

Where r is the rate of the reaction, C is the concentration of the contaminant, t is time, k is the rate constant, Θ is the fraction of the surface covered by the reactant, and K is the adsorption equilibrium constant.

Eq. 2 can be simplified when the concentration is either very high (KC >> 1) or very low (KC << 1). Under conditions of low concentration, KC becomes negligible compared to 1 and Eq. 2 reduces to a first order reaction:

$$-\frac{dC}{dt} = kKC \qquad \text{(Eq. 3)}$$

Similarly, under conditions of high concentration, 1 becomes negligible compared to KC. Eq. 2 reduces to a zero order reaction, where the reaction rate is equal to the rate constant, k. This simplification is illustrated in the photocatalytic degredation of 4-chlorophenol, where no additional increase in rate was observed with an increase in initial concentration above 0.2 millimoles (Al-Ekabi and Serpone, 1989). It was reasoned that at a high enough contaminant concentration, the surface sites of the catalyst are

completely saturated, so further increase in concentration cannot further increase the rate of reaction, according to LH kinetics. Conversely, below the specified concentration, the catalyst surface sites are not completely saturated; therefore, the fraction of the surface covered by the contaminant will vary with concentration, thereby varying the reaction rate.

The applicability of the LH model can be validated by inverting Eq. 2 and plotting 1/r vs. 1/C. The slope of a linear plot provides 1/kK and the 1/k value is given by the y-intercept.

$$-\frac{1}{dC/dt} = \left(\frac{1}{kK}\right)\frac{1}{C} + \frac{1}{k} \qquad \text{(Eq. 4)}$$

This equation has been found to be accurate for the reaction rate in a single component system, with no competition for reactive sites, but must be expanded to accurately describe a multi-component system (Turchi and Ollis, 1989).

Catalyst Supports

The utilization of a photocatalyst as a slurry can be effective, but creates difficulties in recovering the catalyst due to its small particle size. For this reason, the use of a variety of supports, such as glass beads, carbon, sand, clay, and silica gel, have been investigated (Matthews, 1993). There are additional advantages to using a support that is capable of adsorbing the organic contaminants. The rate of destruction is generally controlled by the concentration of the contaminant; therefore, the rate of mineralization will decrease as the contaminant concentration decreases. This makes reducing the concentration of organics to low levels a slow process. If an adsorbent is used as a support, a high concentration of the contaminant is created around the photocatalyst, which increases the rate of mineralization (Yoneyama and Torimoto, 2000). The

adsorbent support can also retain intermediates that are formed during the destruction process. The possibility of creating toxic intermediates during photocatalysis is a concern, but if the intermediates are held near the catalyst they are more likely to be completely destroyed.

Silica gel and activated carbon are two porous media that are being investigated as catalyst supports. Activated carbon is commonly used in water treatment to adsorb undesired organic components. Its proven adsorption capabilities make it a good candidate for a photocatalyst support. An obvious adverse affect of the addition of activated carbon is its opaque nature. The activated carbon could prevent photons from reaching the photocatalyst, decreasing activation and subsequently reducing mineralization. Silica gel generally has a lower surface area than carbon, but has the advantage of being transparent, allowing the light to penetrate and activate the titanium dioxide.

There is some disagreement in the literature as to the level of adsorption desired in the catalyst support. A study of the photocatalytic destruction of propionaldehyde in the air phase revealed that a catalyst support with medium level adsorption abilities compared to the other adsorbents used in the study (carbon having high adsorption and zeolum having low adsorption) showed the fastest degradation (Yoneyama and Torimoto, 2000). The reasoning was based on the longer time needed for diffusion from composites involving strong adsorption. Similarly, it was found that the use of activated carbon as a catalyst support was not advantageous in the destruction of dichloromethane in water (Torimoto et al., 1997). The reason for this result was attributed to slower diffusion of dichlormethane from the adsorbent compared to the bulk solution. However, an

investigation of a single compound, methylene blue, using various activated carbon types as catalyst supports for TiO_2 was completed (Khan, 2003). Here it was found that the stronger adsorbents led to better destruction. Further analysis as to the cause of varied destruction levels resulting from different activated carbon supports revealed that higher metal content led to enhanced photocatalysis. Khan explains that the metals contained in the AC could act as electron acceptors, reducing the recombination of electron/hole pairs and leading to increased photocatalysis.

Activated Carbon

Activated carbon (AC) can be made from a variety of carbonaceous materials, including coal, peat, peanut shells, and wood, which are charred and subsequently activated through a chemical or physical process, such as the application of steam or CO_2 at temperatures typically around 900°C and higher. The final product is a material that has a high surface area (generally 500-1500 m^2/g) and high energy for removing pollutants.

AC is a well-known technology for the removal of organic compounds from water through adsorption. The drawback of AC is that once its adsorption capacity is reached, it must either be replaced or regenerated, a process that usually involves burning off the adsorbed pollutants and a corresponding loss of carbon mass. This drawback could be overcome through a combination of AC and TiO_2. The AC adsorbs the contaminants, leading to more efficient photocatalysis, and the photocatalysis destroys the pollutants, leading to regeneration of the adsorbent. This concept has been investigated by generating composites of AC coated with titanium dioxide (Lu et al., 1999; Torimoto et al., 1996; Torimoto et al., 1997; Yoneyama and Torimoto, 2000; Khan, 2003). The TiO_2 can be coated on the AC through various methods, such as impregnation or boiling

deposition. Different methods will lead to AC-TiO_2 composites with different properties. The disappearance of contaminants as well as the disappearance of total organic carbon has been monitored (Lu et al., 1999; Torimoto et al., 1996) and found that although TiO_2 alone decreased contaminant concentrations at a faster rate, the overall decomposition of the contaminants and intermediates was faster with the AC-TiO_2 composite. This supports the idea that the AC will adsorb the intermediates, holding them close to the photocatalyst until completely mineralized.

Several studies claim enhanced photocatalysis through the addition of AC in an aqueous suspension of TiO_2 (Matos et al., 1998; Herrmann et al., 1999; Matos et al., 2001; Gomes da Silva and Faria, 2003). The location of the degradation process in aqueous suspensions has been studied (Minero et al., 1992) and shows that the oxidation reaction takes place close to the catalyst surface; therefore, the use of the two materials in an aqueous suspension relies on the transfer of the pollutants from the adsorbent to the photocatalyst. This creates an added step compared to the AC-TiO_2 composites; the contaminants must be somehow transferred, possibly during a collision, from the AC to the TiO_2. Two studies directly compared the use of a mixture versus a composite using the same quantity of carbon and TiO_2 in each experiment with the same organic compound (Torimoto et al., 1997; Nagaoka et al., 2002). These authors agreed that enhanced removal occurred with the addition of carbon compared to TiO_2 alone, but found that physically combining the two materials was more advantageous. Torimoto reasons that the photodecomposition of the adsorbed species must take place during collisions, and this occurrence is simply not high enough to compete with the AC-TiO_2 composite. In addition, the aqueous suspension defeats the original purpose of

supporting TiO_2 in the first place, which is to enable the TiO_2 particles to be easily separated from the solution after photocatalysis.

The regeneration of AC-TiO_2 has been studied and shown to be difficult. Regeneration after adsorption of an organic dye, methylene blue, of two composites that differed in the type of AC was studied (Khan, 2003). The first attempt at regeneration of one AC-TiO_2 composite showed a loss of its capacity with each 24-hour regeneration cycle. Khan reasoned that some of the carbon may not be exposed to UV light, preventing photocatalysis; therefore, a second regeneration attempt involved simultaneous fluidization with UV irradiation. This succeeded in regenerating the AC-TiO_2 back to its initial uptake, but the AC-TiO_2 reached exhaustion faster than in the first cycle. The other AC-TiO_2 composite, made with a different AC, was regenerated only through intermittent 12 hour irradiation, but was not restored to its original level.

Another study that focused on the regeneration of AC-TiO_2 also showed long regeneration times (Crittenden et al., 1997). In order to increase the regeneration rate, Crittenden tried heating the AC-TiO_2 during regeneration with the idea that this would increase the desorption rate, which was thought to be a limiting step in the regeneration rate. The regeneration of AC-TiO_2 was found to be only 10% more efficient than the regeneration of the control, which was AC without TiO_2. This indicated that the efficiency was based on simple desorption rather than oxidation of the organic compounds.

Silica

Silica (SiO_2) is a transparent material that can be synthesized through various chemical methods, providing several options for the creation of SiO_2-TiO_2 composites. Synthesis can occur through preparation of the two oxides simultaneously, as one mixed

material, or through deposition of TiO_2 on SiO_2. Sol-gel hydrolysis, coprecipitation, and flame hydrolysis are the most popular mixed oxide methods, while impregnation, chemical vapor deposition, and precipitation are the methods used for supported oxides, though the supported oxide methods have not received as much attention (Gao and Wachs, 1999). Each method will lead to composites with different behaviors based on differences in surface area, pore size, dispersion of TiO_2 on or in the silica, and bonding between the silica and photocatalyst.

SiO_2-TiO_2 composites have been proven successful in the photocatalytic degradation of a variety of organic compounds (Matthews, 1988; Anderson and Bard, 1995; Anderson and Bard, 1997; Xu et al., 1999; Vohra and Tanaka, 2003). In some studies, SiO_2-TiO_2 has been compared directly to bare TiO_2 and shown to be more advantageous for specified compounds (Xu et al., 1999; Anderson and Bard, 1995). Xu and co-workers synthesized particles from a titania sol and silica powder and tested for photocatalytic destruction of acetophenone. SiO_2-TiO_2 was found to be at least 10% more effective than bare TiO_2. This increased destruction was related to higher adsorption of acetophenone and better dispersion of TiO_2 due to the presence of silica. A similar comparison was performed using SiO_2-TiO_2 and bare TiO_2 particles prepared by a sol-gel technique and tested for the removal of rhodamine-6G (Anderson and Bard, 1995). Again, SiO_2-TiO_2 was found to have a faster degradation rate, which was related to the increased adsorption of the contaminant. These studies demonstrate the idea that increasing adsorption will increase the concentration of the contaminant around the TiO_2 and lead to faster destruction of the contaminant.

Regeneration

Multiple studies have been performed that prove the ability of SiO_2-TiO_2 to be used over and over again. Phenol was repeatedly degraded by greater than 99% in a reactor packed with SiO_2-TiO_2 particles (Matthews, 1988). Cycles of adsorption and destruction of phenol were performed four times without loss of capacity. A series of adsorption and destruction tests were also performed using SiO_2-TiO_2 pellets for the photocatalytic degradation of volatile organics (Holmes, 2003). At least ten runs were performed using the same pellets and achieving 80% or more removal of each of the contaminants. No decrease in the system's original photocatalytic ability was observed in the data. SiO_2-TiO_2 pellets are used in four adsorption and destruction cycles for the removal of an organic dye, crystal violet (Londeree, 2002). No decrease in the pellets' performance is shown; in fact, the adsorption ability of the pellets actually increased with each cycle.

Synthesis by Sol-Gel Method

Compared to other synthesis processes, the sol-gel technique is the most widely used based on its potential for control over the textural and surface properties of the final material (Gao and Wachs, 1999). In addition, because this preparation method begins with high purity chemical precursors, it produces high purity, homogeneous materials (Kirk and Othmer, 1991). Starting from a liquid also has the advantage of shaping the material in a mold, making it easier to produce particles of the size and shape needed for a specific application.

A sol is a suspension of colloidal particles dispersed in a liquid. Under the proper conditions, the sol will form a gel, which is a solid network that holds the liquid in its pores. A sol-gel can be formed through a series of hydrolysis and condensation reactions

of alkoxide precursors. Once the gel is formed, it may undergo aging and drying steps to allow the gel to mature to the desired structure and expel the liquid held in its pores.

Commonly used silica precursors are tetra methyl ortho silicate (TMOS) and tetra ethyl ortho silicate (TEOS). The chemical formulas for these silica precursors are $Si(OCH_3)_4$ and $Si(OC_2H_5)_4$ for TMOS and TEOS, respectively. These can be represented by $Si(OR)_4$ in equations 5 and 6. The alkoxide precursor reacts with water in a hydrolysis reaction (Eq. 5) and the silica network begins to form through condensation reactions (Eq. 6). The network continues to grow through polycondensation. Because the alkoxide precursor is not readily soluble in water, an alcohol is generally used as a solvent in the mixing of these reactants. Depending on the precursor, methanol or ethanol is formed as a byproduct of the hydrolysis reaction and water is produced in the condensation reactions.

$$Si(OR)_4 + 4H_2O \rightarrow Si(OH)_4 + 4ROH \qquad \text{(Eq. 5)}$$

$$Si(OH)_4 + Si(OH)_4 \rightarrow (OH)_3Si - O - Si(OH)_3 + H_2O \qquad \text{(Eq. 6)}$$

The rates of the hydrolysis and condensation reactions that begin formation of the gel have a strong impact on the structure of the final material. These reaction rates will vary with temperature, nature of the solvent, type of alkoxide precursor, and nature and concentration of the acid or base (Hench and West, 1990). The acid or base concentration has been shown to be the dominant factor (Orcel, 1987). In general, increasing the concentration of H^+ or H_3O^+ in acidic conditions or increasing the concentration of OH^- in basic conditions will increase the rate of hydrolysis. The ratio of water to the alkoxide precursor, the R ratio, also affects the rate of hydrolysis. Water can be used in excess to promote hydrolysis. The rate of the hydrolysis and condensation

reactions will ultimately affect the gel time and the structure of the gel. Hydrofluoric acid has been used to decrease the gel time and increase the pore size of the resulting gel (Powers, 1998).

After gelation, at which point the three dimensional silica network has formed and the sol ceases to move as a liquid, the polycondensation reactions continue as the silica network further develops. Syneresis and Ostwald ripening also contribute to this aging process. Syneresis involves the contraction of the silica gel network as a result of the condensation reactions, which create additional silica network links and cause more liquid to be expelled. Ostwald ripening describes the formation of the silica gel network in the areas of negative curvature, filling in these crevices on the surface of the silica gel. This process strengthens the gel, which helps to protect the gel against cracking during drying. The time and temperature under which the aging process is allowed to occur will impact the surface area and pore size of the gel.

Alcohol and water produced in the aforementioned reactions remain in the pores of the gel. The gel must be dried, typically at temperatures between 100ºC and 180ºC, to remove the liquid from the pores. Capillary forces are created by the evaporation of the liquid, causing some of the pores to collapse and the gel to shrink. Silica gels dried in this manner are termed xerogels and will generally be reduced in volume by 40-60% (El Shafei, 2000). Steps can be taken to reduce the amount of shrinking and create a silica gel of higher surface area and pore volume. One method involves replacing the water with a liquid of lower surface tension, such as an alcohol, before drying. A gel can also be supercritically dried to completely eliminate the destructive forces of surface tension, minimizing the amount that the gel shrinks.

Silica Gel Properties

The silica network consists of four oxygen atoms bonded to each silicon atom, forming a tetrahedron, and each oxygen atom is shared by two silicon atoms. These Si-O-Si, or siloxane, bonds make up the bulk silica structure. The surface of the silica is hydroxylated in the presence of water, forming Si-OH, or silanol, groups. It is these silanol groups that make the silica surface hydrophilic and determine the reactivity of the silica (El Shafei, 2000). The silanol groups can be defined as single, geminal, or vincinal. Single silanol groups are isolated and formed with a silicon atom that is bonded to three other oxygen atoms in siloxane bonds. When at a close enough distance, the hydroxyl groups can interact with each other through hydrogen bonding, creating vincinal silanols. Geminal silanols exist when two hydroxyl groups are linked to the same silicon atom. The silica surface can be dehydroxylated through heating above temperatures of 200ºC. The silanol groups will condense to form siloxane bonds. Dehydroxylation will occur at a greater degree as the temperature is increased.

In the presence of water, the silanol groups become ionized and the hydrogen atom will associate or dissociate depending on the pH of the solution (Icenhower and Dove, 2000). The point of zero charge (PZC) of silica is between a pH of 2 and 3; therefore, at pH values above this PZC, the hydrogen atoms will begin to dissociate. This deprotonation will leave a negative charge on the surface of the silica (Eq. 7).

$$Si\text{-}OH \leftrightarrow Si\text{-}O^- + H^+ \qquad \text{(Eq. 7)}$$

Silica-Carbon Composites

Combining silica and carbon can potentially combine the advantages of each material to create a composite with improved adsorption capabilities. These composites may possess a heterogeneous surface through combination of the properties of the

nonpolar, hydrophobic carbon with the polar, hydrophilic silica to create a material that can adsorb both inorganic and organic contaminants (Skubiszewska-Zieba, 2002). Carbon-silica composites have been successfully created through several methods, including pyrolysis of methylene chloride on the surface of silica gel (Villieras et al., 1998), pyrolyzed elutrilithe in a sol-gel (Deng et al., 1998), and coating of silica gel on the carbon surface through hydrolysis of a silica precursor (Cheong et al., 2003). Deng showed that combining the carbon and silica created a composite with different adsorption capacities than the individual materials. For certain adsorbates, namely water, cyclohexane, acetone, and pyridine, carbon-silica composites had superior uptake when compared to silica or carbon alone (Deng et al., 1998). Composites consisting of carbon, silica and titanium dioxide have also been generated for the epoxidation of cyclohexene (Cheong, 2003). The titanium dioxide supported by both carbon and silica was found to provide greater conversion of cyclohexene compared to titanium dioxide support by silica or carbon alone. The advantages of each material were successfully combined: the carbon provided higher selectivity for the epoxide due to its hydrophobic nature, and the silica provided a better environment for catalytic activity.

CHAPTER 3
MATERIALS AND METHODS

SiO_2-TiO_2 Composites

The SiO_2-TiO_2 composites were created using a sol-gel method (Londeree, 2002). The silica precursor was tetra-ethyl-ortho-silicate (TEOS) (Fisher Scientific, reagent grade). It was mixed with nanopure water using a water to TEOS mole ratio of 16:1. Ethanol (Aaper Alcohol, 200 proof) was used as the solvent to facilitate the miscibility between the TEOS and water. Two acid catalysts were used: a 1 M nitric acid solution, made from 15.8 M nitric acid (Fisher Scientific, certified A.C.S.) and nanopure water, and a 3% solution of hydroflouric acid, formulated from 49% hydrofluoric acid (Fisher Scientific, reagent A.C.S.) and nanopure water. Table 1 summarizes the quantity of each chemical used to make one batch, approximately 10 g, of silica gel. The volume of hydrofluoric acid was varied to control the pore size of the gel. Volumes of 2, 3, and 4 mL correspond to approximate pore diameters of 70, 118, and 234 angstroms, respectively.

Table 1. Chemicals Used for Silica Gel Synthesis

Chemical	Volume
Nanopure water	25 mL
Ethanol	50 mL
TEOS	35 mL
1 M Nitric Acid	4 mL
3% Hydrofluoric Acid	2-4 mL

The chemicals in Table 1 were mixed in polystyrene containers in the order listed using a magnetic stir plate. While mixing, the liquid was doped with the desired quantity

of Degussa P25 TiO_2. According to Degussa, the TiO_2 possesses the properties listed in Table 2.

Table 2. Properties of Degussa P25 TiO_2

Property	Value
Specific surface area (BET)	50 +/- 15 m2/g
Average primary particle size	30 nm
Tapped density	130 g/L
pH value in 4% dispersion	3.5-4.5

For the composites that included activated carbon, the mixture was doped with activated carbon after the addition of TiO_2. The activated carbon used in the composites was ground to an average particle diameter between 1 and 2 microns as determined by the LS2 13 320 Laser Diffraction Particle Size Analyzer. The distribution of the particle size is shown in Figure 2.

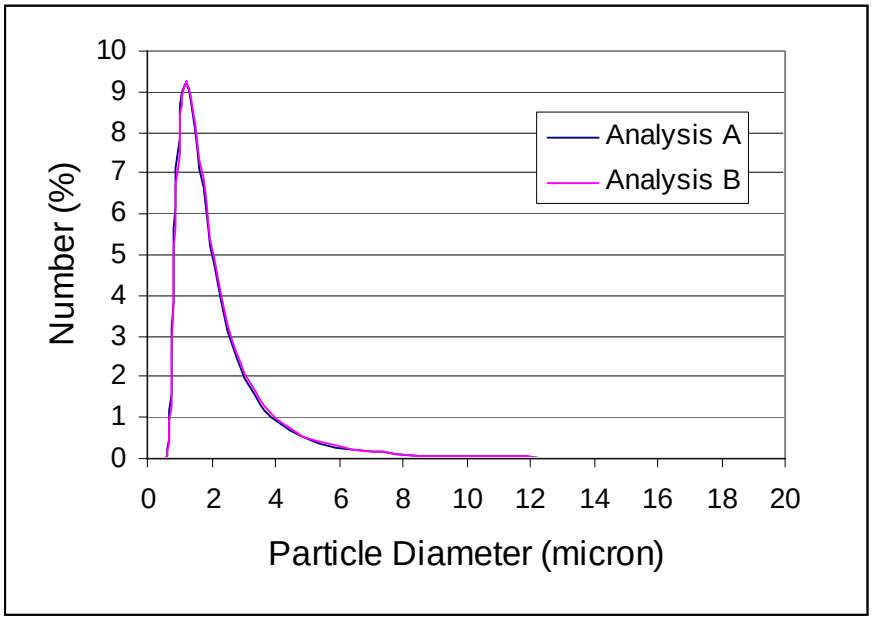

Figure 2. Particle size distribution of activated carbon used in AC-SiO_2-TiO_2 composites. Analysis A and Analysis B are duplicates of the particle size distribution analysis.

The TiO_2 and activated carbon loadings stated throughout this document are referred to as percentages. The TiO_2 loadings are reported on a basis of TiO_2 weight per TEOS volume. For example, the 12% TiO_2 loading is determined using 4.2 g of TiO_2 per 35 mL of TEOS as a percentage. The activated carbon loadings are reported by a weight percentage using the activated carbon mass per total mass of the pellets.

The sol was allowed to mix between 0.5 and 7 hours, depending on the amount of 3% HF used. For the amounts of 2, 3, and 4 mL, approximate mixing times of 7, 2, and 0.5 hours were used, respectively. The liquid was then transferred to 96-well assay plates and allowed to gel (Figure 3). The assay plates were Fisherbrand, polystyrene plates that contained 0.45 mL in each well.

Figure 3. Silica sols doped with titanium dioxide were mixed using magnetic stir plates and transferred to 96 well assay plates before forming a gel.

Upon reaching the gel point, at which point the sol no longer moved as a liquid, the trays were capped and wrapped in aluminum foil to prevent any of the contents from volatilizing during the aging process. The gels were aged for 48 hours at room temperature and 48 hours at 65°C in an Oakton Stable Temperature oven. After aging, the pellets were removed from the assay plates and transferred into Teflon screw cap jars.

Each lid had a small hole to allow the liquid expelled from the gel's pores to slowly escape as vapor during the drying process. The drying process involved heating at 103ºC for 18 hours and 180ºC for 6 hours in a Yamato DVS 400 Drying Oven. The BET (Brunauer, Emmett, and Teller equation) surface areas and pore volumes of the gels were analyzed using a Quantachrome NOVA 1200 Gas Sorption Analyzer.

Reactor System

The pellets were packed into a cylindrical reactor (Figure 4). The reactor was designed with a hollow center and thin annulus to allow the UV lamp to be placed in the center, providing maximum UV light exposure to the pellets. The inner wall of the annulus was a quartz tube that could be completely removed, making it simple to remove the pellets after testing. The lamp in the center of the quartz tube provided UV light at a wavelength of 365 nm. As measured at the center of the lamp, the intensity was 7.4 mW/cm^2 at the inner diameter of the annulus and decreased to 5 mW/cm^2 at the outer diameter. Specifications of the reactor are listed in Table 3. The reactor was enclosed in a box to provide control over its exposure to ambient light.

Figure 4. Reactor packed with SiO_2-TiO_2 composites with a UV light through the center.

Table 3. Reactor Specifications

Specification	Value
Length of Reactor	19 cm
Inner Diameter	2.5 cm
Outer Diameter	4.2 cm
Empty Bed Volume of Pellets	138.6 mL

The system consisted of the reactor, 6 mm PTFE tubing, a Masterflex L/S Digital Standard Drive peristaltic pump, and a reservoir of simulated wastewater (Figure 5). The system was used in two different configurations. One system configuration allowed the wastewater to pass through the reactor only once, and the other formed a closed loop system in which the wastewater was recirculated through the reactor. A cover (not shown in figure 5) was placed over the front of the reactor to completely enclose it during operation of the system. The reservoir was a one liter flask that was covered with aluminum foil to prevent any outside UV light exposure and capped with parafilm to create a closed system.

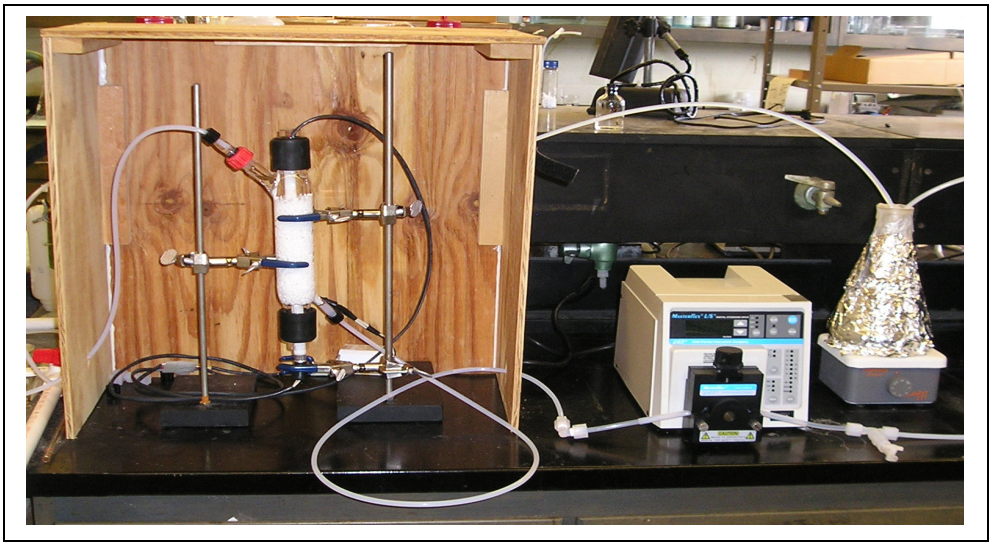

Figure 5. Treatment system consisting of reactor packed with SiO_2-TiO_2 composites, UV lamp, pump, and reservoir of simulated wastewater.

Simulated Wastewater

The wastewater feed was created using a formula for typical wastewater provided by Johnson Space Center (JSC). The chemical composition includes the shower waste, hand wash waste, oral hygiene waste, urine, and urine flush waste that would be expected from a crew of four people. Table 4 lists the amounts of each constituent present in the simulated wastewater.

Table 4. Simulated Wastewater Composition

Wastewater Component	Quantity
Pert Plus for Kids	1.2 g
Deionized water	999.4 ml
Ammonium bicarbonate, NH_4HCO_3	2726 mg
Sodium chloride, NaCl	850 mg
Potassium bicarbonate, $KHCO_3$	378 mg
Creatinine, $C_4H_7N_3O$	248 mg
Hippuric acid, $C_9H_9NO_3$	174 mg
Potassium dihydrogen phosphate, KH_2PO_4	173 mg
Potassium bisulfate, $KHSO_4$	111 mg
Citric acid monohydrate, $C_6H_8O_7 \cdot H_2O$	92 mg
Tyrosine, $C_9H_{11}NO_3$	66 mg
Glucuronic acid, $C_6H_{10}O_7$	60 mg
1.48N Ammonium hydroxide, NH_4OH	10 ml

This formula represents the raw wastewater that would be the influent for the beginning of the water treatment system; therefore, it would be treated by several processes before actually becoming the feed for the post-processor. To account for pretreatment, the simulated wastewater is diluted using 9 mL of the concentrated solution with 991 mL of deionized water to make each liter of wastewater feed. This creates a solution of approximately 3 ppm of total organic carbon (TOC), which is within the range of the TOC concentration expected of the post processor influent (Cambel et al., 2003). It was found that the wastewater was not stable over long periods of time, particularly at room temperature. The liquid would change in color, from a cloudy, white mixture to

yellow, and the TOC concentration decreased over time. Therefore, a new solution of the concentrated wastewater was created each week and stored in an amber bottle at 4ºC. A small fraction of the wastewater was found to be volatile, so the wastewater feed was mixed for approximately 1 hour before use to allow the volatiles to be removed and the TOC concentration to stabilize.

Reactor Dynamics

A tracer analysis was conducted to determine the behavior of the reactor. Sodium chloride was chosen as a tracer because it was not expected to be adsorbed by the media and had been used successfully as a tracer in a previous study (Holmes, 2002). The sodium chloride concentration was measured using conductivity measurements read by a Fisher Scientific conductivity probe. A linear correlation between conductivity and sodium chloride concentration was observed and used to translate conductivity measurements to a sodium chloride concentration (Figure 6).

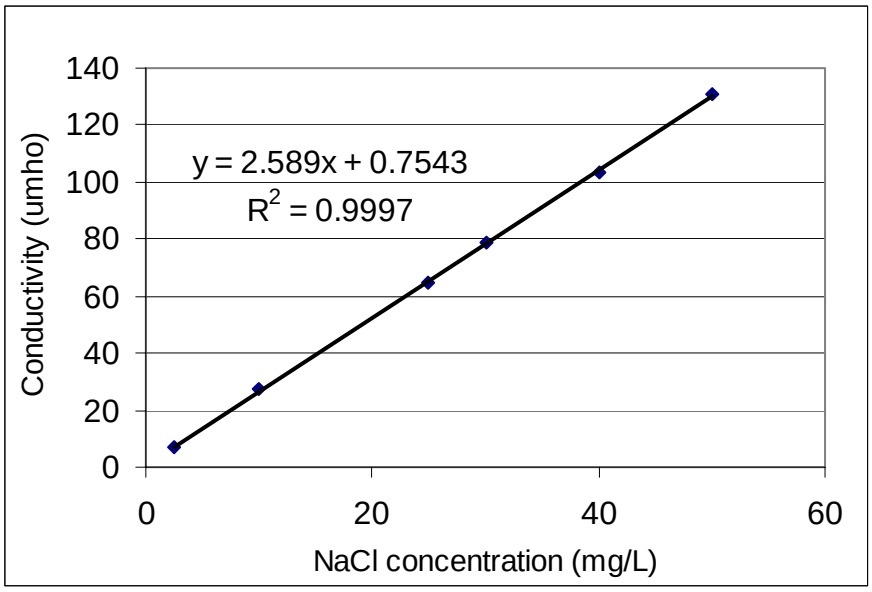

Figure 6. Calibration of conductivity meter

DI water was pumped through the reactor until a stable conductivity was achieved. For the tracer analysis, this conductivity was subtracted from effluent readings to determine the sodium chloride concentration exiting the reactor. The tracer analysis was performed two ways to provide a duplicate study. First, a solution of 50 mg/L sodium chloride was pumped through the reactor and the conductivity of the effluent was monitored until the concentration of the effluent reached 50 mg/L. A second experiment was conducted in which DI water was pumped through the reactor and the effluent conductivity was monitored until it indicated that all the sodium chloride had been washed out of the reactor. The flow rate used for both tests was 10 mL/min.

The data collected from the tracer analysis were used to calculate a mean residence time and to model the reactor behavior. The mean residence time was determined to be 12.5 minutes. A fractional age distribution (E-curve) of the sodium chloride in the reactor was created for both reactor tests. This distribution was then compared to that of the model of continuously stirred tank reactors (CSTRs) in series to determine the number of tanks in series the reactor behavior was approximately equivalent to (Figures 7 and 8). The E-curve for the CSTR-in-series model was created using Eq. 8.

$$E = \frac{n e^{\frac{-nt}{\bar{t}}}}{\bar{t}(n-1)!}\left(\frac{nt}{\bar{t}}\right)^{n-1} \qquad \text{Eq. 8}$$

Where n is the number of CSTRs in series, t is the time in the reactor, and t_{bar} is the mean residence time.

A comparison of the data with the CSTR-in-series model reveals that the reactor behaves as five CSTRs in series.

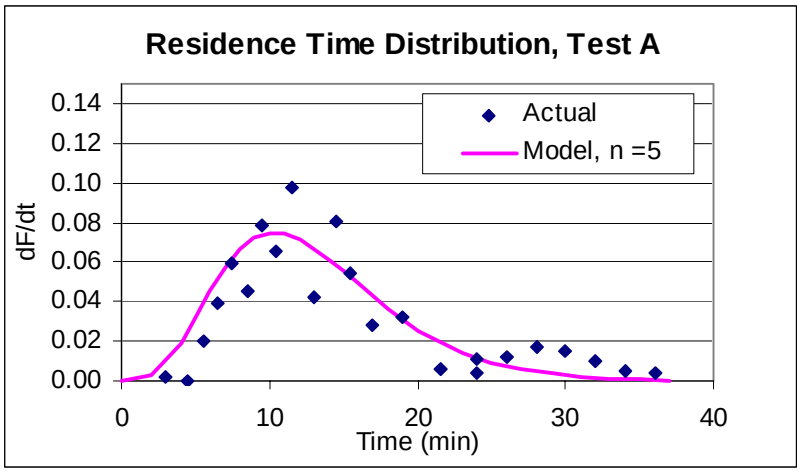

Figure 7. This figure compares the residence time distribution of the reactor as compared to a CSTR-in-series model. Test A was performed by pumping 50 mg/L of NaCl through the reactor until the effluent reached the same concentration.

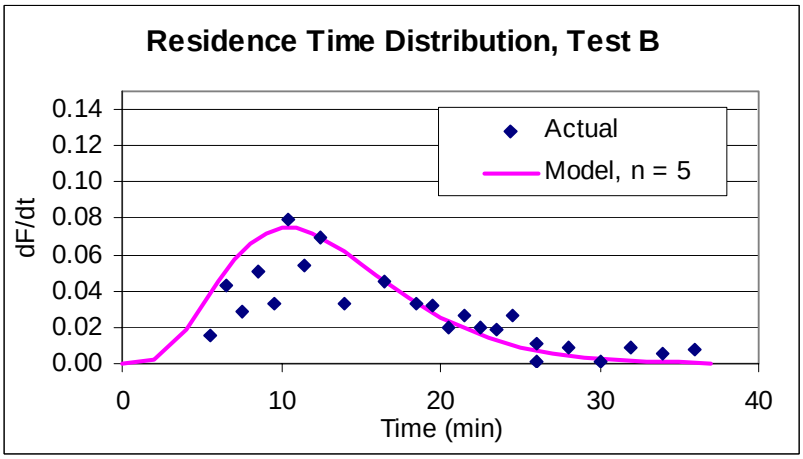

Figure 8. This figure compares the residence time distribution of the reactor as compared to a CSTR-in-series model. Test B was performed by pumping DI water through the reactor until the NaCl concentration decreased from 50 mg/L.

Experimental Procedures

Adsorption and Destruction

In order to optimize the system, experiments were performed to test its sensitivity to flow rate, pore size of the silica gel support, titanium dioxide loading, and addition of activated carbon to the catalyst support. With each change to the system, removal of TOC achieved by adsorption and destruction was quantified. All samples were analyzed using a Tekmar Dohrmann Apollo 9000 combustion analyzer.

The amount of pellets packed in the reactor was measured by volume as 115 mL in a 100 mL graduated cylinder and held constant for each experiment. The regeneration ability and effects of the experiments on the pellets was unknown; therefore, the reactor was packed with new pellets for each experiment. Because of the acidic properties of the silica gel, all pellets were pre-washed with a sodium hydroxide solution (pH = 8.5) to reduce the pH changed caused by the pellets. The pellets were washed until a pH of 4 was reached in the effluent stream.

To study TOC removal by adsorption, wastewater was first pumped through the reactor in a single-pass configuration, in the dark, until the pellets were exhausted, meaning that the influent TOC concentration equaled the effluent TOC concentration. After the adsorption capacity had been reached, the system, including the reactor and tubing, remained full of 264 mL of wastewater and the reservoir was filled with 1 liter of wastewater. The wastewater was recirculated and the UV lamp was turned on. Because the pellets were previously exhausted with respect to TOC adsorption, TOC removal during this experiment was assumed to be due to destruction. Samples of 25 mL were taken from the reservoir every few hours until the TOC concentration reached below 500 ppb.

Because the pellets were still acidic, even after a period of washing, the pellets changed the pH of the wastewater as it flowed through the reactor. For the single pass adsorption experiments, the pH was decreased from 8 at the influent to 6 at the effluent. Recirculation of the wastewater for the destruction tests decreased the initial pH of 8 to a final pH of 4. The pH of the influent and effluent was monitored in all experiments using

a Fisher Scientific pH meter and these pH changes remained consistent throughout all the tests.

Adsorption of Intermediates

Experiments were performed to test the adsorption of the intermediates formed after UV exposure in the reactor at different empty bed contact times (EBCTs), which is defined as the time needed for one bed volume of water to pass through the reactor (calculated using the empty bed volume divided by the flow rate). The pre-washed pellets in the reactor were first exhausted in the dark. The UV light was then turned on and the effluent was collected in a reservoir. This experiment was performed at flow rates of 5, 10, 20, and 30 mL/min. A 1 inch glass tube packed with 65 mL of pre-washed pellets was used to test the adsorption of the effluent. In each case, the adsorption experiment was performed at a flow rate of 10 mL/min with a new set of pellets and conducted immediately following collection of the effluent. A diagram of the apparatus is shown in Figure 9.

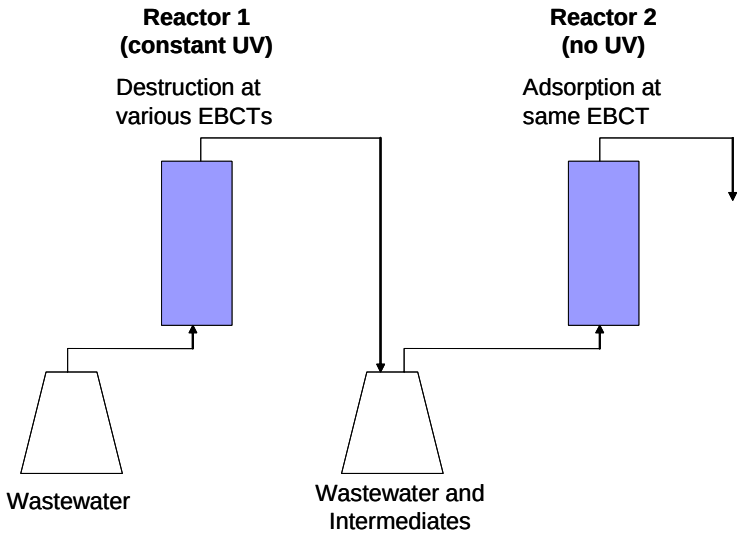

Figure 9. Diagram of the system used to test the adsorption of the intermediates formed from photocatalysis at different EBCTs.

CHAPTER 4
RESULTS

System Optimization

The photocatalytic system was optimized with respect to flow rate, pore size of the silica support, titanium dioxide loading, and activated carbon loading. For each test of the system, one parameter was varied while the others were held constant. The adsorption and destruction abilities of the system were tested at each set of conditions. The optimum system parameters were chosen based on the ability to reduce the TOC concentration to 500 ppb in the shortest amount of time. The wastewater concentration is represented in all graphs as a normalized TOC concentration, showing the fraction of the effluent TOC concentration (C_e) over the influent TOC concentration (C_0, 3 ppm). The pellet pore sizes reported in this results section are approximate; the BET surface area, pore volume, and calculated pore size of each pellet composition that was tested can be found in the Appendix.

Flow Rate

Flow rate was the first parameter to be varied. Experiments were performed using flow rates of 5, 10, 20, and 30 mL/min, which are of the appropriate order of magnitude to treat the wastewater produced by 1-4 crew members per day. A flow rate of 16 mL/min would provide treatment for wastewater produced by 2 people per day, assuming a production of 11.5 L of wastewater per crew member (Campbell et al., 2003). The SiO_2-TiO_2 pellets used to test each flow rate had a 12% TiO_2 loading and pore size of 118 angstroms. The system was first operated in a single pass configuration with no UV light

to test the adsorption behavior of the pellets. The results are displayed in Figure 10. The adsorption curves at each flow rate are compared directly using bed volumes as the independent variable. Figure 10 shows that lower flow rates lead to lower effluent concentrations in the first few bed volumes. The lower flow rates create longer EBCTs, allowing more time for diffusion of the wastewater through the pores of the silica and then subsequent adsorption. The 5, 10, and 20 mL/min flow rates cause exhaustion of the pellets after approximately 6 bed volumes, while the pellets tested at the 30 mL/min flow rate reach exhaustion sooner, at 3 bed volumes.

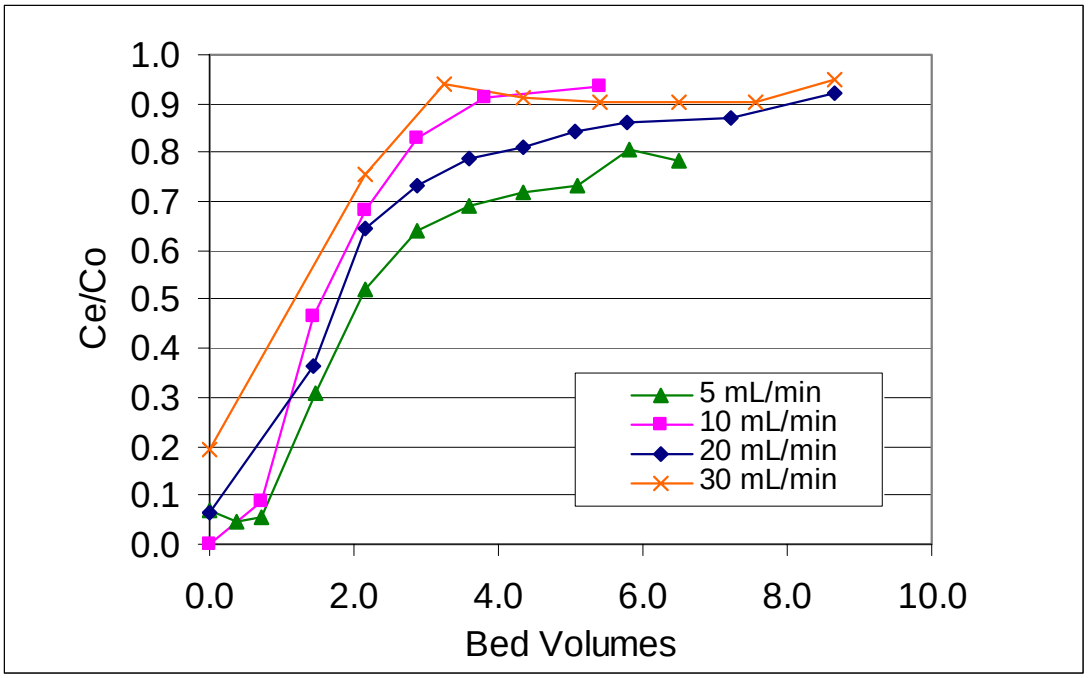

Figure 10. TOC removal by adsorption at flow rates of 5, 10, 20, and 30 mL/min, corresponding to EBCTs of 28, 14, 7, and 5.25 minutes and hydraulic loading rates of 0.55, 1.1, 2.2, and 3.3 cm^3/cm^2-min, respectively.

After the pellets were exhausted, or close to exhaustion, the system was reconfigured from a single pass to a recirculating mode, with constant UV light exposure in the reactor. Because the pellets were previously exhausted, it was assumed that TOC removal during this testing period was due to complete mineralization. Figure 11 shows

that the rate of destruction depends on the flow rate, with the 20 mL/min flow rate reaching below the desired 500 ppb in the shortest amount of time. Despite the fact that the pellets tested at 5 mL/min were not entirely exhausted, meaning that some of the removal during the destruction period could be due to adsorption, the destruction test conducted at 5 mL/min required the longest time to reach 500 ppb. This is surprising, since the slower flow rates are shown to allow more time for the contaminants to adsorb, and increased adsorption was expected to lead to increased destruction.

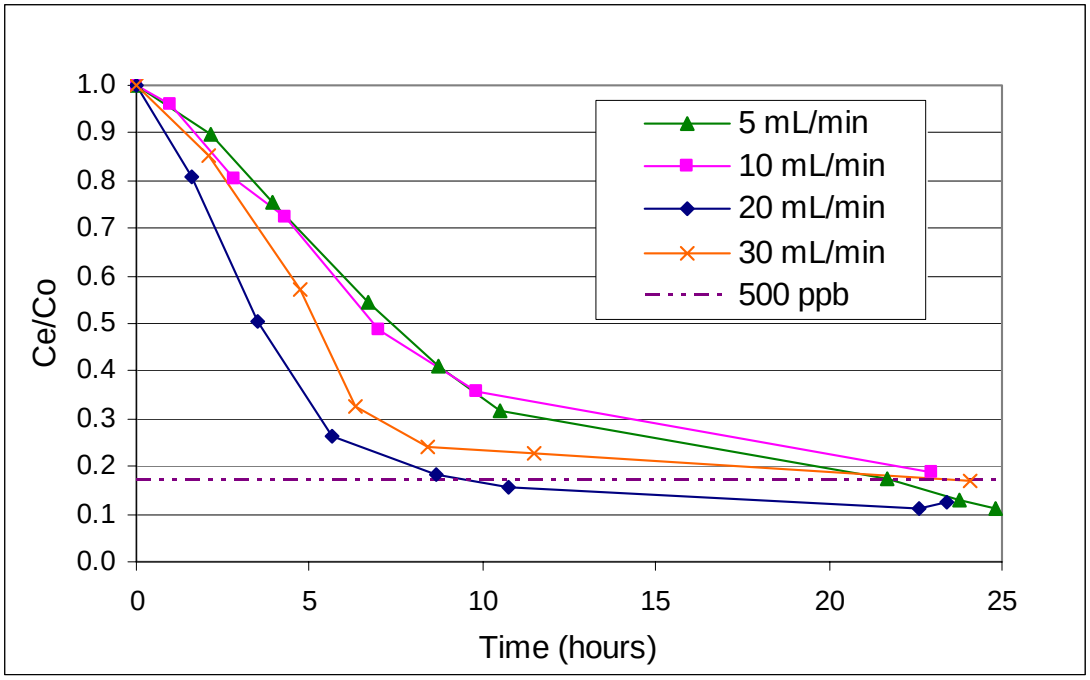

Figure 11. TOC removal by destruction in a recirculating system at flow rates of 5, 10, 20, and 30 mL/min, corresponding to EBCTs of 28, 14, 7, and 5.25 minutes and hydraulic loading rates of 0.55, 1.1, 2.2, and 3.3 cm^3/cm^2-min, respectively.

It is important to realize that the recirculation means that the total time the wastewater is in the reactor is approximately equal, regardless of the flow rate. For example, at a flow rate of 20 mL/min, the wastewater might pass through the reactor 4 times as fast compared to a 5 mL/min flow rate, but it would also experience 4 times as

many passes. Therefore, one of the differences between the flow rates is that the wastewater spends intermittent time in the reactor at the higher flow rates compared to longer, continuous passes through the reactor at slower flow rates. It is possible that different intermediates, or quantity of intermediates, are created at different EBCTs, which could change the adsorption of the wastewater after the first pass through the reactor.

In order to test the adsorption of the intermediate wastewater (i.e., wastewater and intermediates created after contact with the irradiated SiO_2-TiO_2 composites), the wastewater was first passed through the reactor with constant UV light at a certain EBCT. Then, the effluent from the first reactor was passed through a second reactor, which was in the dark, to test for adsorption of these intermediates. The EBCT of the first reactor was varied to create effluents equivalent to that after a single pass through the reactor at the flow rates used during the recirculating destruction test. The EBCT in the second reactor was held constant so that the adsorption of the various wastewater effluents could be directly compared. Figure 12 presents the adsorption curves for the intermediate wastewater created from the single pass through the second reactor. The data show no difference in the adsorption of the wastewater after passing through the reactor at different EBCTs. Therefore, the better performance at 20 mL/min shown in Figure 11 did not result from the formation of intermediates that were more adsorbable.

A second hypothesis based on diffusion of the wastewater was formulated to explain the variation in the destruction rates as the flow rate was changed. The rate of destruction depends on the ability of the contaminants to reach the titanium dioxide in the porous surface of the pellets and the ability of the products resulting from the oxidation

reactions to travel out of the pores. It is possible that the higher flow rates increase the diffusion of the molecules in and out of the pellets. The transport of the wastewater contaminants and the photocatalysis products in and out of the pellets' pores depends on several steps. These steps include transport through the bulk solution, transport through the film layer formed by stationary water surrounding the pellet, and travel through the pores. Higher flow rates decrease the film layer surrounding the pellet; thus, decreasing the distance the molecules must diffuse to approach the pellet surface. While higher flow rates were shown to have a negative impact on adsorption behavior in a single pass system, the impact of higher flow rates on the adsorption behavior of intermediate products as well as the transport of final products out of the pores and into the bulk solution is unknown.

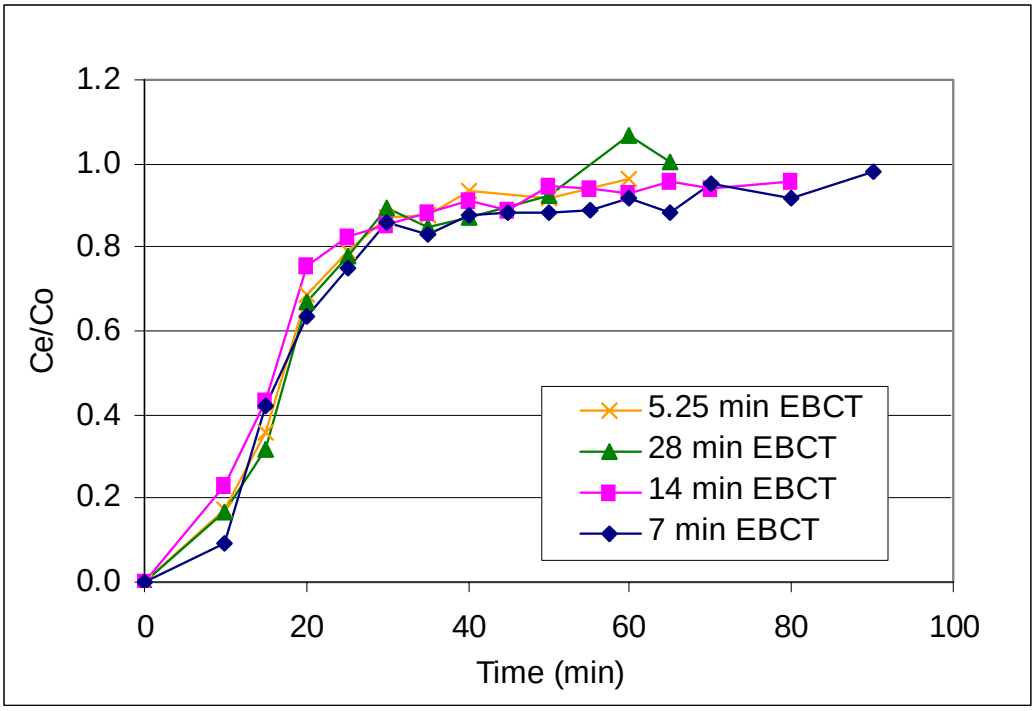

Figure 12. TOC removal by adsorption of wastewater effluents resulting from destruction at various EBCTs.

In order to test the hypothesis of diffusion being a limiting factor in the system, pellets of the same composition but approximately half the size (smaller diameter, same length) were tested using a flow rate of 20 mL/min. If diffusion were a limiting factor, the expectation was that the smaller pellets would increase the bulk surface area and decrease the distance a contaminant must travel inside the pellet, leading to a faster destruction rate. The results presented in Figures 13 and 14 show that the smaller pellets performed worse than the original size pellets. These data indicate that diffusion is not the limiting factor controlling the destruction rate. It is possible that changing the size of the pellets also changed another system parameter, such as the light penetration or the hydraulic flow through the reactor, which decreased the destruction rate of the system.

Pore Size

Using the optimum flow rate of 20 mL/min and the same 12% TiO_2 loading, the pore size was varied to determine its effect on the adsorption and destruction capabilities of the system. Figure 15 shows the adsorption curves for three different pore sizes: 70, 118, and 234 angstroms.

The surface area of the gels decreased with increasing pore size. The 234 angstrom gel, with the lowest surface area, exhibited the worst adsorption, exhausting at 4 bed volumes. All the curves show exhaustion of the pellets by 8 bed volumes, indicating that only a small amount of adsorption is occurring with any of the three pore sizes. This is not unexpected since the surface of the silica gel is hydrophilic, and the contaminants being adsorbed are hydrophobic. In addition, the adsorption is occurring at a pH of 6, which is well above silica's isoelectric point of 2-3; therefore, the surface of the silica is likely to be negatively charged. The main ingredient in the wastewater is soap, which is an anionic surfactant, and some of the other organics are carboxylic acids, which will also

form anions when dissociated. Charge repulsion could also be a reason for the low adsorption.

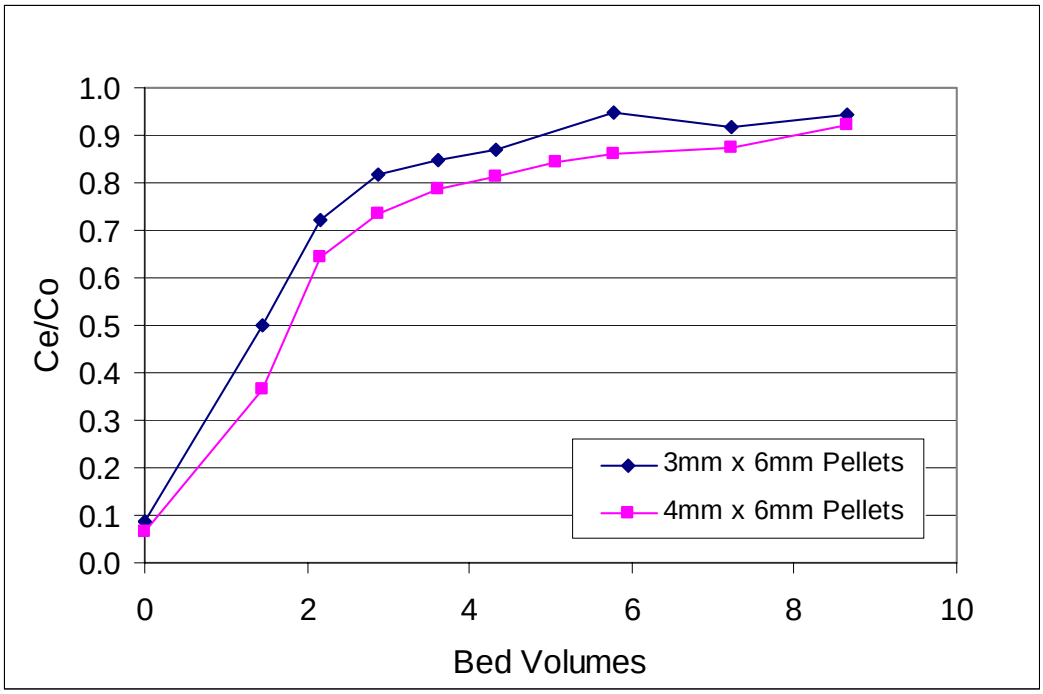

Figure 13. Effect of pellet size on adsorption of the wastewater.

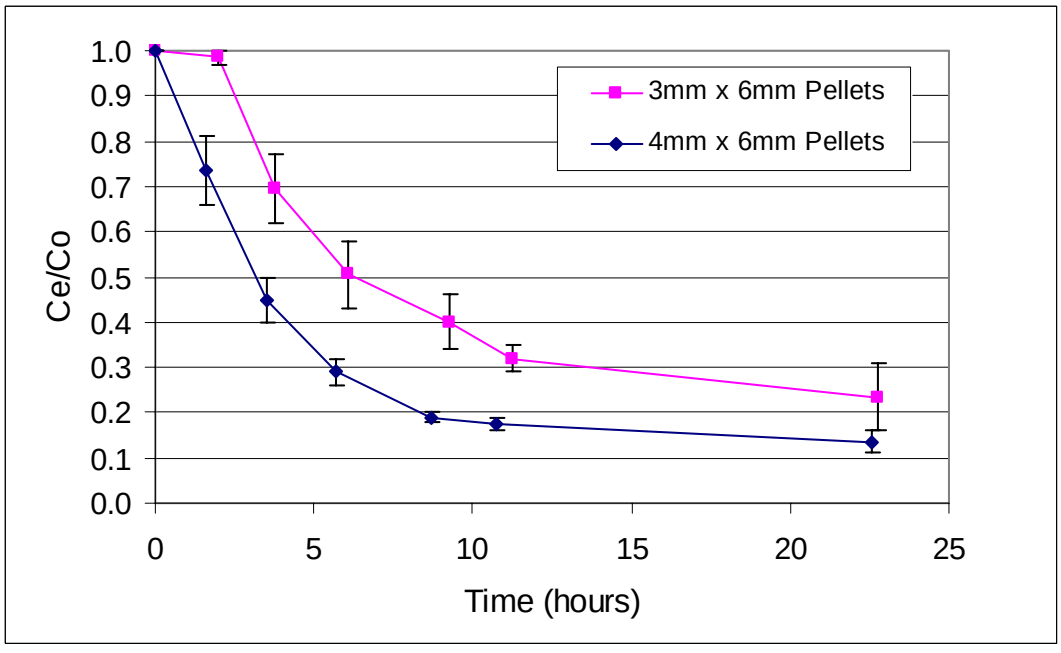

Figure 14. Effect of pellet size on destruction of the wastewater.

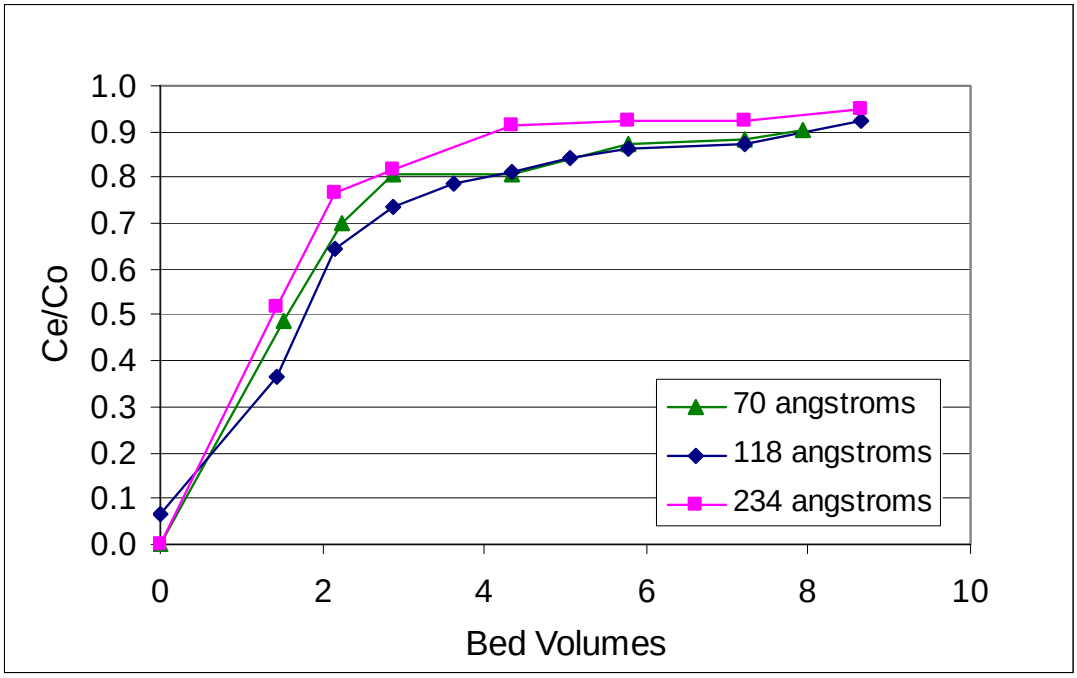

Figure 15. Effect of pore size on adsorption of the wastewater.

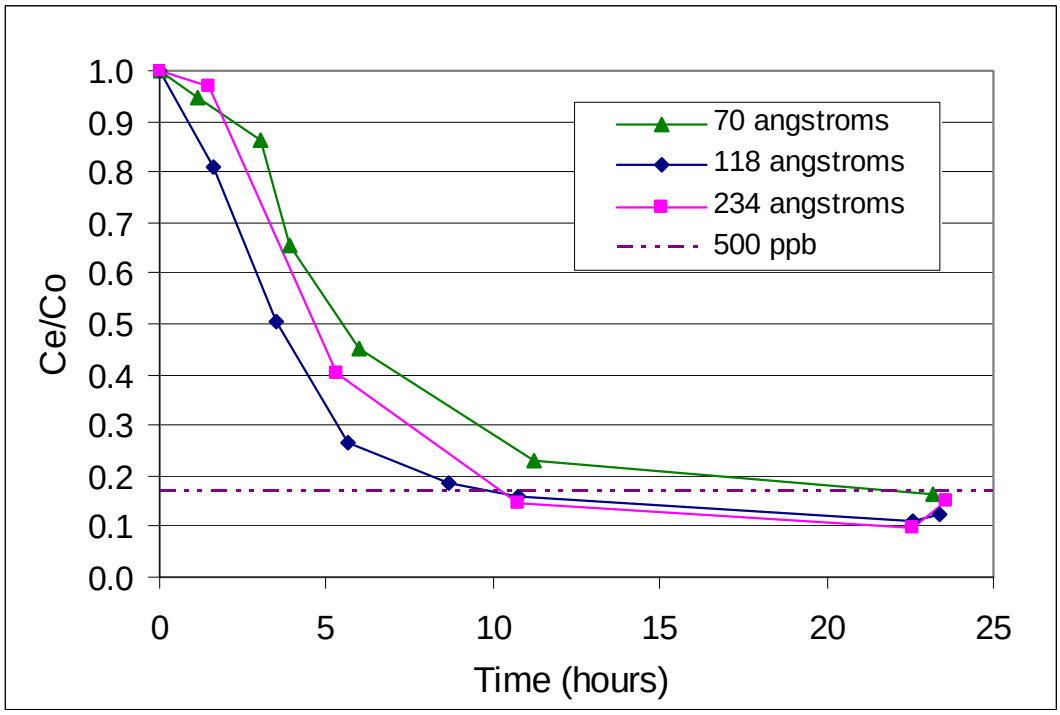

Figure 16. Effect of pore size on the destruction of the wastewater.

The results of the destruction test are displayed in Figure 16. The 118 angstrom composite performs better than the composite with a 234 angstrom pore size, which could be due to the higher adsorption of the 118 angstrom composite as shown in Figure 15. Although the 70 angstrom composite shows adsorption behavior similar to the 118 angstrom composite, it displays the slowest destruction rate of all three pore sizes. The 70 angstrom pore size could be too small to allow adequate diffusion of the molecules in and out of the pores. The middle pore size of 118 angstroms shows the fastest destruction of the three pore sizes tested, possibly due to the best combination of adsorption and diffusion, and was chosen as the optimum pore size for future experiments.

Titanium Dioxide Loading

The TiO_2 loading was varied while keeping the chosen flow rate and pore size constant. TiO_2 loadings of 0, 3, 12, 24, and 32% (% by weight of TiO_2/volume of TEOS) were tested and compared (Figures 17 and 18). A clear trend is not observed in the adsorption curves of pellets with various TiO_2 loadings. The pellets show similar adsorption, with only the 24% TiO_2 loading exhibiting a slight decrease in adsorption, exhausting about 15 minutes before the other pellets. The destruction curves presented in Figure 18 show the best performance with a TiO_2 loading of 12%. The test of the composite with no TiO_2, only SiO_2, serves as a control, showing the destruction that occurs in the system through photolysis alone. The curve shows that approximately 20-30% of the TOC is able to be removed without the addition of TiO_2 to the system.

The 12% TiO_2 is significantly better than the 3% loading, showing that more catalyst is needed in the system for faster destruction; however, further increase past 12% TiO_2 does not greatly improve the destruction rate of the system. The 24% loading

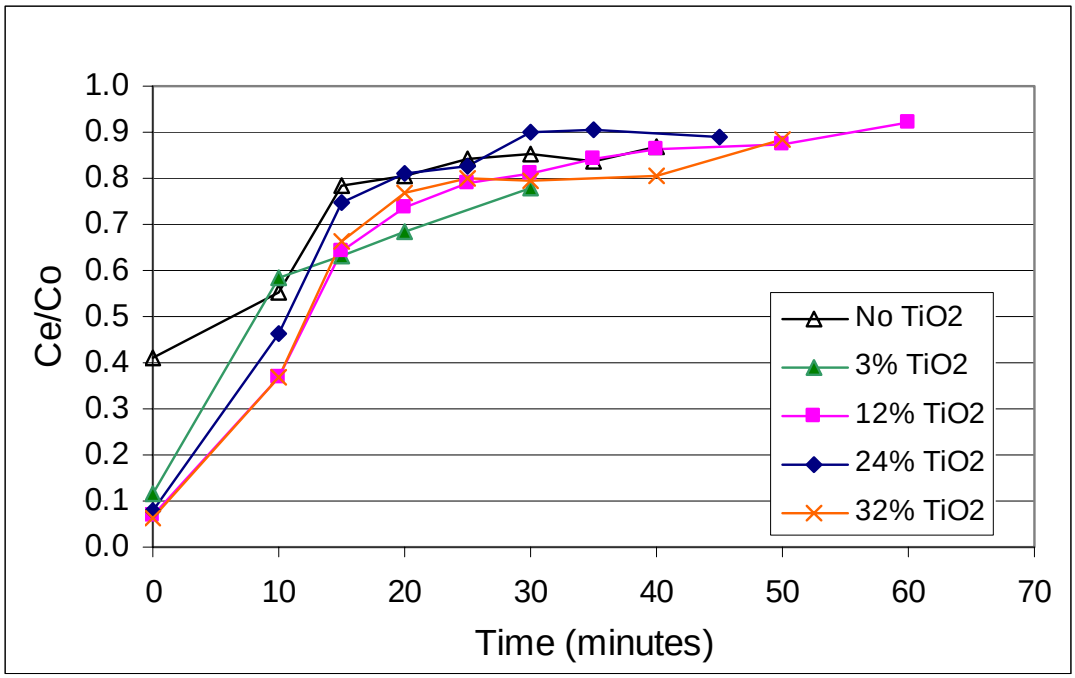

Figure 17. Effect of TiO_2 loading on adsorption of the wastewater.

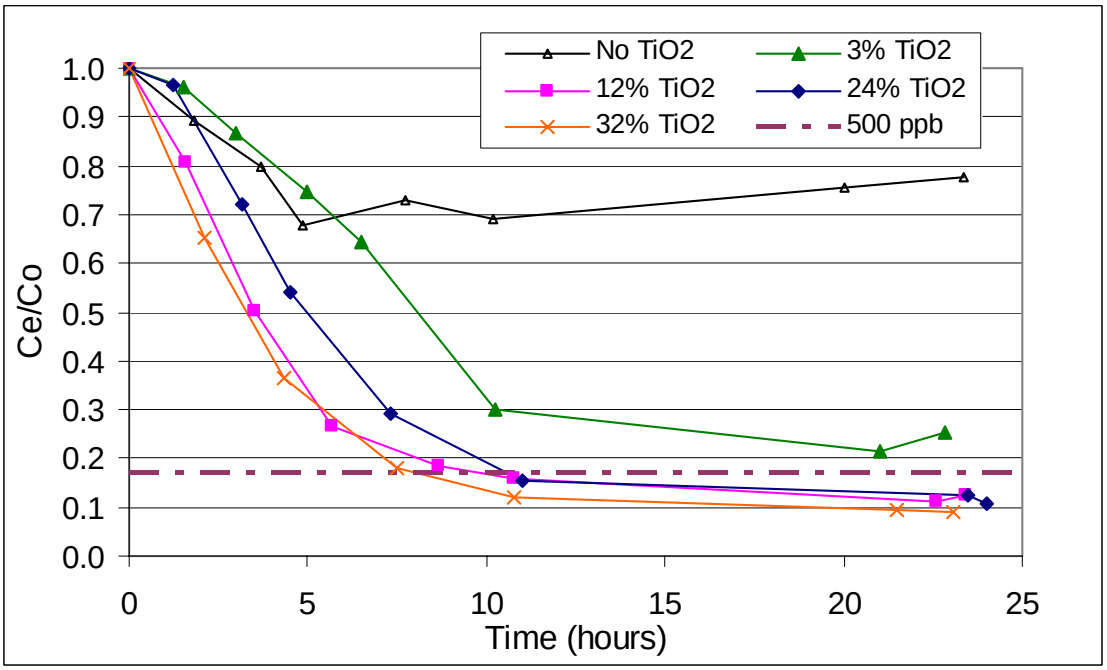

Figure 18. Effect of TiO_2 loading on destruction of the wastewater.

actually exhibits slower degradation, and the 32% loading decreased the TOC concentration to 500 ppb about an hour sooner than the 12% loading. It is possible that there is a limit to the amount of TiO_2 that can be effectively dispersed near the surface of the silica gel, and at higher loadings the TiO_2 will agglomerate and some of the TiO_2 will be blocked from the UV light. The 32% TiO_2 pellet shows that the addition of more TiO_2 can lead to better performance; however, 2.5 times the amount of TiO_2 in the 12% TiO_2 composite was required to decrease the destruction time by approximately 20%. Because this level of improvement in the destruction rate does not justify such a large increase in TiO_2 loading, the 12% TiO_2 loading was chosen as the optimum TiO_2 loading.

Activated Carbon Loading

Activated carbon was added to the SiO_2-TiO_2 pellets to explore its effect on the performance of the system. It was expected that the adsorption of the organic contaminants would increase, but it was difficult to predict the effects on the system's destruction abilities. The increased adsorption could enhance the destruction rate, but the activated carbon could also have a negative impact on the system by blocking the UV light needed to activate the catalyst. In order to find the optimum activated carbon loading that increased adsorption without blocking too much UV light, several different activated carbon loadings were tested at two different TiO_2 loadings of 12% and 24%. The increase in adsorption with the addition of activated carbon to pellets of 24% TiO_2 is illustrated in Figure 19. The time needed to exhaust the pellets doubles with even the lowest activated carbon loading, 1.3wt%.

The destruction performance of the pellets containing activated carbon is compared to pellets without any carbon in Figure 20. It is interesting to find that in the two lowest carbon loadings, 1.3wt% and 2.6wt%, the carbon addition had no impact on the time

needed to reach the 500 ppb TOC limit. At the higher loading of 3.9wt%, the carbon begins to negatively impact the destruction rate, most likely due to blocking of UV light needed to activate the catalyst.

Because practical operation of the system would involve exhaustion of the carbon in the dark, destruction of the organics under constant UV, and then repeating, the cycle, it was important to test the ability of the activated carbon to be used again. For this reason, an additional adsorption test was conducted after the usual adsorption and destruction cycle. The second adsorption cycle showed complete regeneration for the 1.3% and 3.9% activated carbon loadings (Figures 21 and 22). Regeneration was not tested for the 2.6% carbon loading.

The effect of activated carbon addition was also tested with a 12% TiO_2 loading. A higher carbon loading of 9.6wt% was explored, and the results are shown in Figures 23 and 24. It is clear that the 9.6wt% greatly increases the adsorption of the organic contaminants. After more than 6 hours, the system was not yet exhausted. The destruction test shows that the carbon does inhibit the destruction rate, though the concentration still reaches the necessary 500 ppb level.

Because the carbon was exhausted only to a C_e/C_0 ratio of 0.6, it is possible that the some of the removal shown in Figure 24 was due to adsorption. A second adsorption experiment was conducted after the destruction cycle to determine if the carbon had been regenerated. Figure 25 shows complete regeneration of the carbon. The regeneration displayed in Figure 25 indicates that destruction was also occurring, and enough of the organic contaminants were destroyed to clean the surface of the activated carbon.

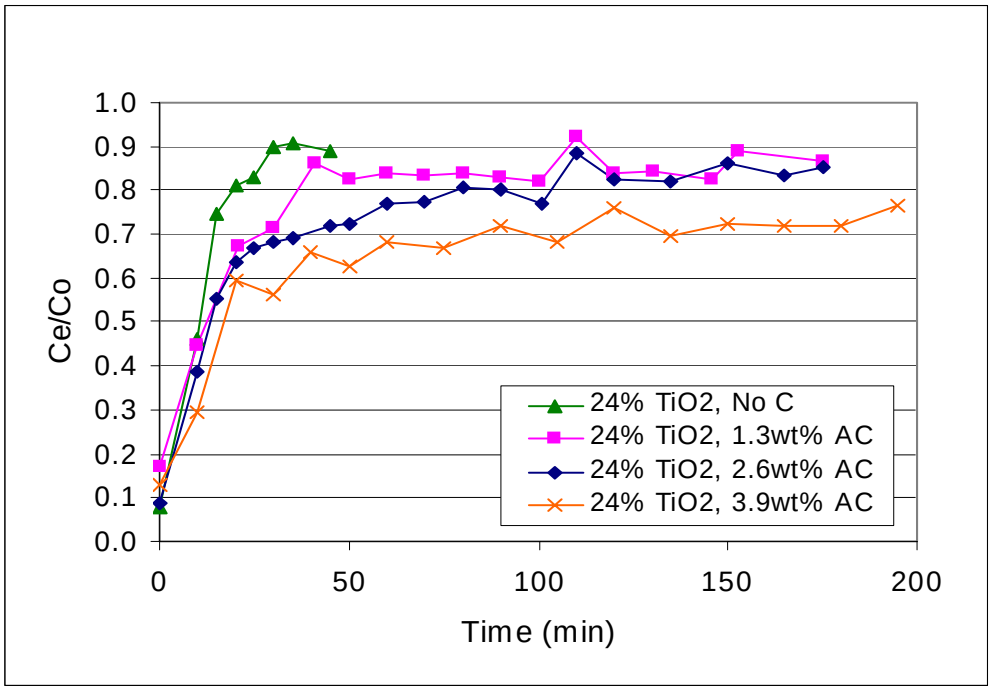

Figure 19. Effect of activated carbon addition to the adsorption properties of the pellets.

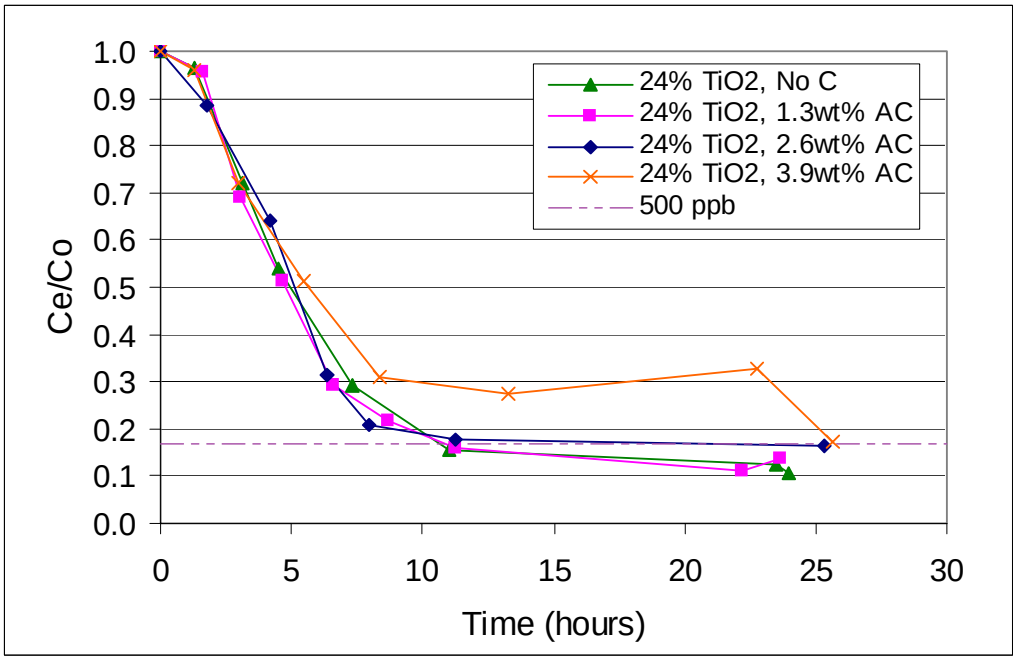

Figure 20. Effect of activated carbon loading on the destruction performance of the pellets.

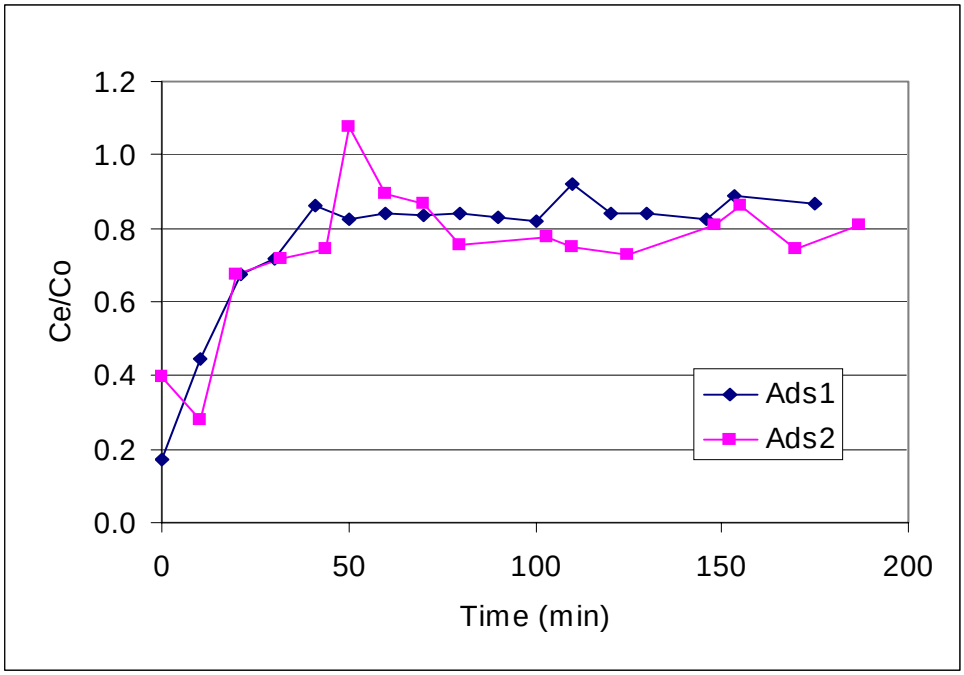

Figure 21. Comparison of the first adsorption cycle (ads1) to the adsorption of the pellets after the destruction cycle (ads2), using pellets of 24% TiO2 loading, 118 angstroms, and 1.3wt% activated carbon loading.

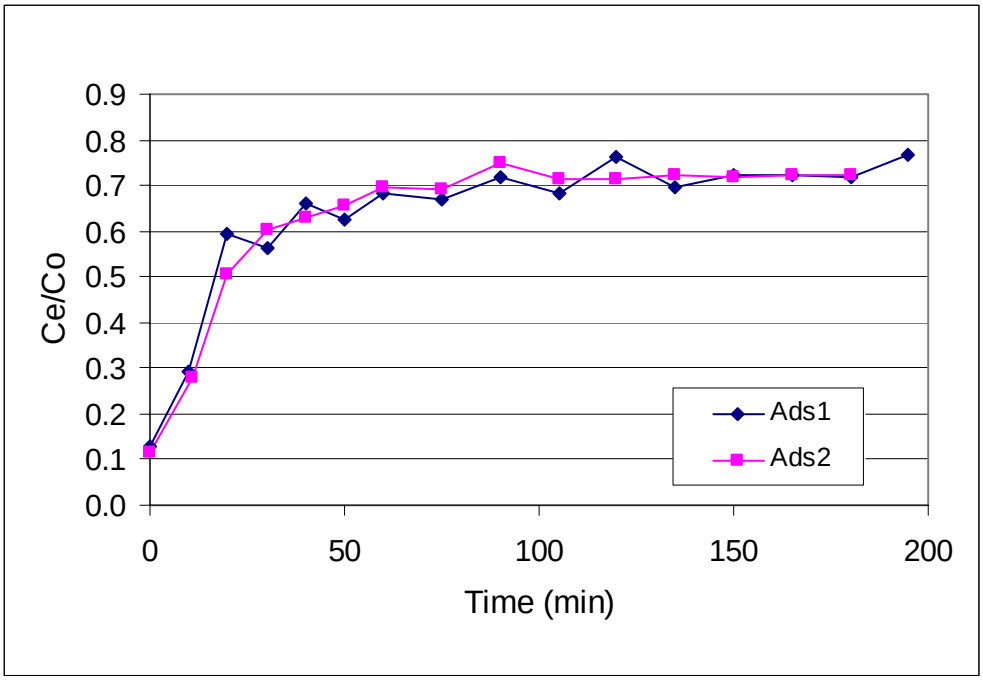

Figure 22. Comparison of the first adsorption cycle (ads1) to the adsorption fo the pellets after the destruction cycle (ads2), using pellets of 24% TiO2 loading, 118 angstroms, and 3.9wt% activated carbon loading.

Similar to the trend in the 3.9wt% carbon loading in Figure 20, the destruction curve for the 9.6wt% carbon shows an increase in the TOC concentration to a C_e/C_0 ratio of 0.3 just before decreasing to 500 ppb. It is possible that this phenomenon seen in the destruction tests of the highest activated carbon loadings could be due to desorption of the organics from the carbon. Because the destruction cycle is performed following exhaustion of the pellets, the pellets with higher activated carbon loadings have more organic contaminants contained in the pores at the start of the destruction test. It is possible that as the TOC concentration of the contaminants in solution decreases to a certain level, some of the contaminants held within the pores desorb into solution before becoming completely mineralized.

The advantage of the activated carbon addition is the increase in the adsorption cycle with the ability to regenerate the carbon surface, meaning that the system could be operated in repeated cycles of adsorption and destruction. The increased adsorption properties allow longer periods in the absence of UV light, which decreases the energy requirements of the system. When considering this type of system operation, the 2.6wt% exhibits the most potential compared to the other activated carbon loadings that were tested. Although the 3.9% and 9.6% loadings were shown to require the longest times to reach exhaustion, creating longer dark periods, the destruction periods were lengthened by more then double, increasing the time requiring the presence of UV light by about 15 hours. The destruction period was the same for the composites containing zero, 1.3%, and 2.6% activated carbon loading. Of these three composite compositions, the composite containing 2.6% carbon is the best choice because it exhibited the longest period of adsorption.

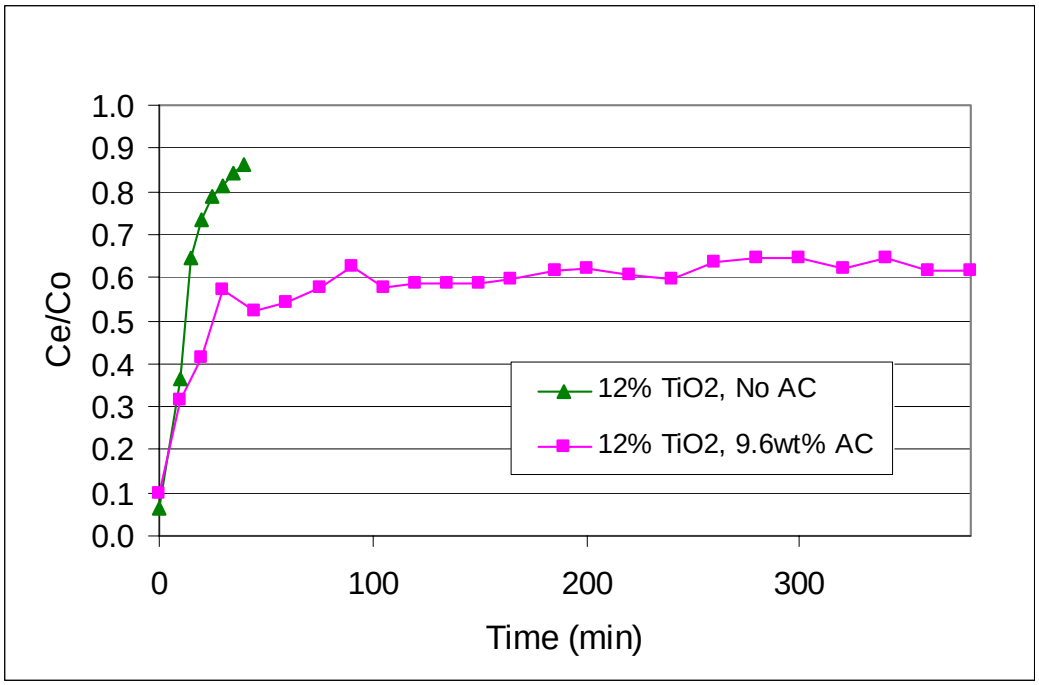

Figure 23. Effect of activated carbon loading on the adsorption properties of the pellets.

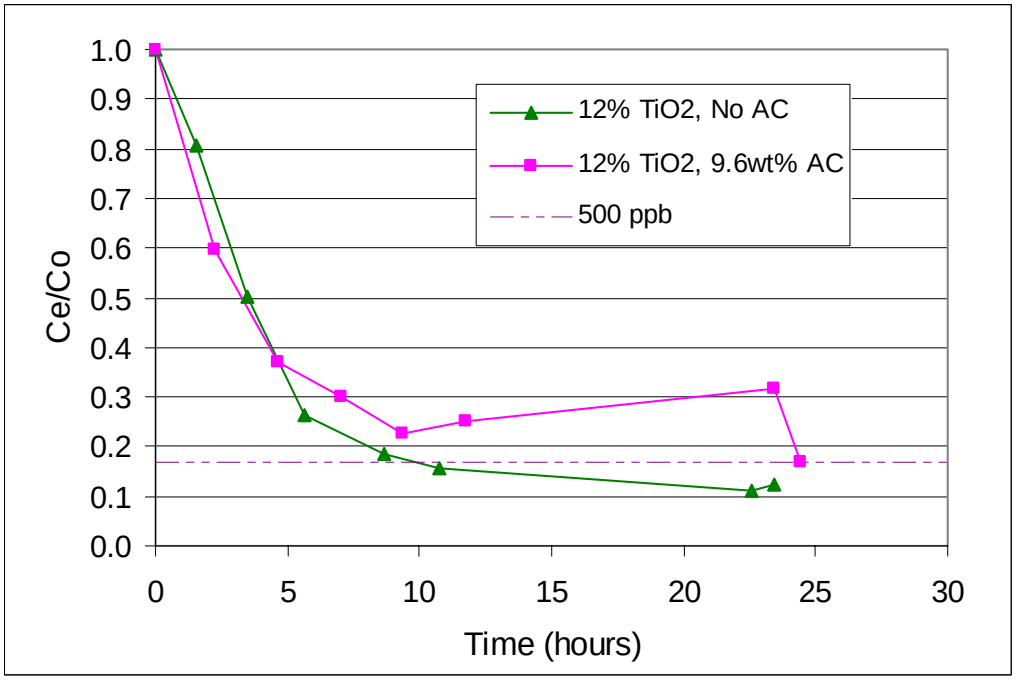

Figure 24. Effect of activated carbon loading on the destruction performance of the pellets.

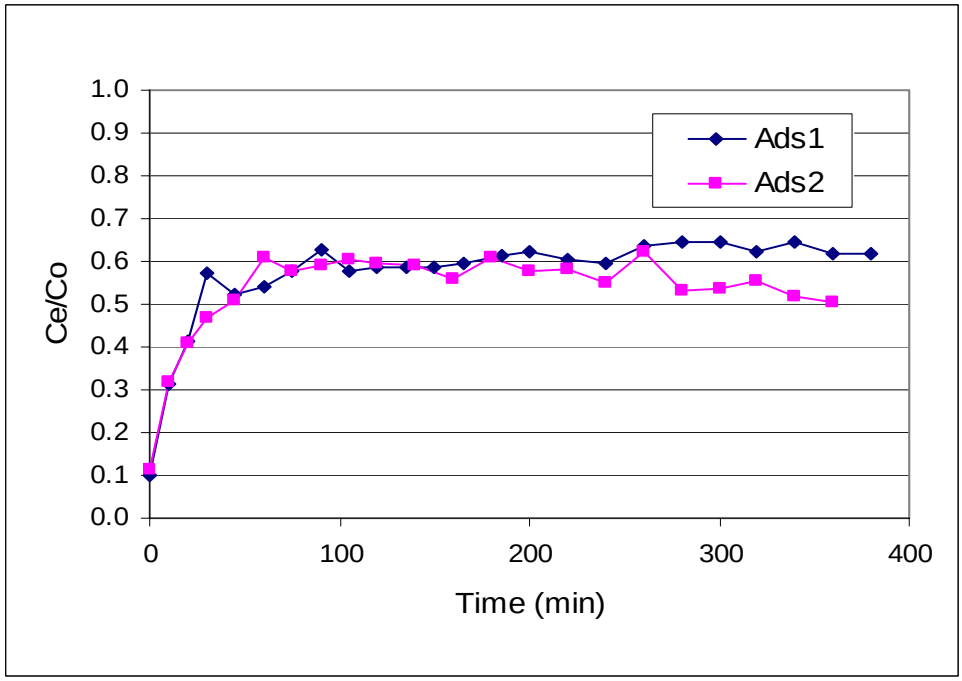

Figure 25. Comparison of the first adsorption cycle (ads1) to the adsorption of the pellets after the destruction cycle (ads2), using pellets of 12% TiO2 loading, 118 angstroms, and 9.6wt% activated carbon loading.

Kinetics

The rate constants for the destruction performance at each set of system conditions were calculated using LH kinetics. It was assumed that the concentration was low enough to reduce the LH equation to a first order reaction, although no experiments were performed to verify first order behavior. Using the number of CSTRs in series, n, determined through the tracer analysis to be 5, and assuming a first order reaction, the equation for the effluent concentration at any particular time, t, is described by the following equation:

$$C_e = C_0\left(1+\frac{kt}{n}\right)^{-n} \qquad \text{Eq. 9}$$

where k is the rate constant. In this discussion, the k values that are calculated describe the destruction behavior of the photocatalytic system and represent the product

of the rate constant and the equilibrium adsorption constant, or the kK term shown in the reduced LH equation (Eq. 3).

The time each plug of wastewater spent in the reactor was estimated for use in Eq. 9. This time was calculated from the time at which the destruction curve crossed the 500 ppb threshold. The k constants resulting from these calculations are shown in Table 5. The rate constants quantify the optimum choice for each system property: 20 ml/min flow rate, 118 angstrom pore size, and 12% TiO_2 loading. For the TiO_2 loading, the 32% loading actually provides the highest destruction rate, but it is only slightly higher than the 12% loading. Because the 32% loading requires 2.5 times the weight of TiO_2 in the system to reach the higher destruction rate, the 12% TiO_2 loading is considered optimum.

The rate constants for the composites containing activated carbon are also displayed in Table 5. Because the composites containing activated carbon have a higher adsorption capacity than composites without activated carbon, more organic carbon will be held in the pores of the composite at the of the adsorption period. This increase in the amount of organic carbon contained within the composite signifies a higher quantity of TOC in the system at the start of the destruction period. It is important to consider the additional organic carbon that was photocatalytically degraded as well as the longer dark adsorption periods when comparing the kinetics of the composites containing activated carbon. The 2.6% activated carbon composite shows the same rate constant as the composite with a lower activated carbon loading, but it would allow for a longer dark adsorption period; therefore, the 2.6% activated carbon loading is considered the best choice out of the activated carbon loadings that were tested.

Table 5. Rate Constants for TOC Mineralization to 500 ppb

Flow Rate (mL/min)	*Avg. Time in Reactor (min)*	*k (min^{-1})*
5	128.8	0.017
20	56.4	0.038
30	143.4	0.015
Pore Size (angstroms)		
60	133.5	0.016
140	56.4	0.038
320	59.3	0.036
Titanium Dioxide Loading (%)		
3	>148.3	<0.014
12	56.4	0.038
24	62.3	0.034
32	47.5	0.045
Activated Carbon Loading (%)		
1.3% (24% TiO_2)	62.3	0.034
2.6% (24% TiO_2)	83.1	0.034
3.9% (24% TiO_2)	148.3	0.014
9.6% (12% TiO_2)	148.3	0.014

CHAPTER 5
SUMMARY AND CONCLUSION

SiO_2-TiO_2 composites were tested for their ability to photocatalytically degrade the organic contaminants in gray water. The composites were tested in a packed-bed reactor, and the system was optimized with respect to flow rate, TiO_2 loading, and pore size of the SiO_2-TiO_2 composite. Activated carbon was also added to the composites and the effect on the performance of the system was investigated.

The SiO_2-TiO_2 composites were successful in photocatalytically degrading the gray water influent in a recirculating system to a TOC concentration below the 500 ppb maximum limit. The optimum pore size and TiO_2 loading were found to be 118 angstroms and 12% (wt/vol), respectively. The system performed best when operated at a flow rate of 20 mL/min. Activated carbon was found to be capable of improving the overall system performance through increased adsorption, which decreases the energy requirements of the system.

It was hypothesized that increasing the adsorption of the SiO_2-TiO_2 composites would increase the destruction rate of the system. Adsorption was shown to be an important system parameter, but increasing adsorption did not always lead to a better destruction rate. The performances of the 234 angstrom composite and the 30 mL/min flow rate condition illustrate situations where adsorption became a limiting factor and the decreased adsorption led to slower destruction. However, adsorption was not always the limiting factor. Adsorption was increased by lowering the flow rate to 5 mL/min and by adding activated carbon. In each of these cases, other factors, such as UV light exposure,

were affected and the destruction rate did not improve. Adsorption is one of several factors that must be considered in order to optimize the system performance.

APPENDIX
SILICA-TITANIA COMPOSITE CHARACTERIZATION

The BET surface area and pore volume were measured for each composite that was tested. The average pore size was calculated from the following equation (Powers, 1998):

$$R = 2V_p/SA$$

where r is the pore radius, V_p is the specific pore volume and SA is the specific surface area. The measurements for each composite are listed in Table A-1.

Table A-1. Surface Area, Pore Volume, and Pore Size of Composites Tested

Test	TiO_2 Loading	Carbon Loading	BET SSA (m^2/g)	Pore Volume (cm^3/g)	Planned Pore Size (angstroms)	Calculated Pore Size (angstroms)
Flow Rate						
5 mL/min	12%	None	274.5	0.854	140	124
20 mL/min, Test A	12%	None	292.0	0.714	140	98
20 mL/min, Test B	12%	None	259.9	0.871	140	134
Small Pellets, Test A	12%	None	274.0	0.828	140	121
Small Pellets, Test B	12%	None	309.9	0.871	140	112
Average			282.1	0.828		118
Max			309.9	0.871		134
Min			259.9	0.714		98
Pore Size						
60 ang	12%	None	393.6	0.690	60	70
320 ang	12%	None	136.7	0.800	320	234
TiO_2 Loading						
24%	24%	None	263.7	0.770	140	117
32%	32%	None	275.1	0.640	140	93
Activated Carbon Loading						
1.3%	24%	1.3%	256.9	0.682	140	106
2.6%	24%	2.6%	285.0	0.865	140	121
3.9%	24%	3.9%	241.6	0.649	140	107
9.6%	12%	9.6%	317.0	0.809	140	102

LIST OF REFERENCES

Al-Ekabi H, Serpone N. Kinetic studies in heterogeneous photocatalysis. 1. Photocatalytic degradation of chlorinated phenols in aerated aqueous solutions over TiO_2 supported on a glass matrix. Journal of Physical Chemistry, 1988, 92, 5726-5731.

Al-Ekabi H, Serpone N. Kinetic studies in heterogeneous photocatalysis. 2. TiO2-Mediated degradation of 4-chlorophenol alone and in a three-component mixture of 4-chlorophenol, 2, 4-dichlorophenol, and 2,4,5-trichlorophenol in air-equilibrated aqueous media. Langmuir, 1989, 5, 250-255.

Anderson C, Bard A. An improved photocatalyst of TiO_2/SiO_2 prepared by a sol-gel synthesis. Journal of Physical Chemistry, 1995, 99, 9882-9885.

Anderson C, Bard A. Improved photocatalytic activity and characterization of mixed TiO_2/SiO_2 and TiO_2/AlO_3 materials. Journal of Physical Chemistry B, 1997, 101, 2611-2616.

Campbell M, Finger B, Verostko C, Wines K, Pariani G, Pickering K. Integrated Water Recovery System Test. International Conference on Environmental Systems, July, 2003.

Cheong H, Kang K, Rhee H. Preparation of titanium-containing carbon silica composite catalysts and their liquid-phase epoxidation activity. Catalysis Letters, 2003, 86, 1-3, 145-149.

Crittenden J, Suri R, Perram D, Hand D. Decontamination of water using adsorption and photocatalysis. Water Research, 1997, 31, 3, 411-418.

Deng X, Yue Y, Gao Z. New carbon-silica composite adsorbents from elutrilithe. Journal of Colloid and Interface Science, 1998, 206, 52-57.

Diebold U. The surface science of titanium dioxide. Surface Science Reports, 2003, 48, 53-229.

Ding Z, Hu X, Yue P, Lu G, Greenfield P. Synthesis of anatase TiO_2 supported on porous solids by chemical vapor deposition. Catalysis Today, 2001, 68, 173-182.

El Shafei G. Silica surface chemical properties. Adsorption on Silica Surfaces. E. Papirer, Ed. Surfactant Science Series, 2000, 90, 35-61.

Gao X, Wachs I. Titania-silica as catalysts: molecular structural characteristics and physico-chemical properties. Catalysis Today, 1999, 51, 233-254.

Gomes da Silva C, Faria JL. Photochemical and photocatalytic degradation of an azo dye in aqueous solution by UV irradiation. Journal of Photochemistry and Photobiology A: Chemistry, 2003, 155, 133-143.

Hench L, West J. The sol-gel process. Chemical Review, 1990, 90, 33-72.

Herrmann JM, Matos J, Disdier J, Guillard C, Laine J, Malato S, Blanco J. Solar photocatalytic degradation of 4-chlorophenol using the synergistic effect between titania and activated carbon in aqueous suspension. Catalysis Today, 1999, 54, 255-265.

Hoffmann M, Martin S, Choi W, Bahnemann D. Environmental applications of semiconductor photocatalysis. Chemical Review, 1995, 69-96.

Holmes F. The performance of a reactor using photocatalysis to degrade a mixture of organic contaminants in aqueous solution. Master's Thesis, University of Florida, 2003.

Icenhower J, Dove P. Water behavior at silica surfaces. Adsorption on Silica Surfaces. E. Papirer, Ed. Surfactant Science Series, 2000, 90, 280.

Khan A. Titanium dioxide coated activated carbon: A regenerative technology for water recovery. Master's Thesis, University of Florida, 2003.

Kirk R, Othmer D. Sol-gel technology. Kirk-Othmer Encyclopedia of Chemical Technology, 4th Ed. J. Kroschwitz, M Howe-Grant, Eds. New York: Wiley, 1991, 22, 497.

Lange KE, Lin CH. Advanced Life Support Program: Requirements Definition and Design considerations. Document #CTSD-ADV-245 (REV A) presented for the Crew and Thermal Systems Division in Houston, TX.

Liu T, Cheng T. Effects of SiO2 on the catalytic properties of TiO_2 for the incineration of chloroform. Catalysis Today, 1995, 26, 71-77.

Londeree D. Silica-titania composites for water treatment. Master's Thesis, University of Florida, 2002.

Lu M, Chen J, Chang K. Effect of adsorbents coated with titanium dioxide on the photocatalytic degradation of propoxur. Chemosphere, 1999, 38, 3, 617-627.

Matos J, Laine J, Herrmann JM. Synergy effect in the photocatalytic degradation of phenol on a suspended mixture of titania and activated carbon. Applied Catalysis B: Environmental 1998, 18, 281-291.

Matos J, Laine J, Herrmann JM. Effect of the type of activated carbons on the photocatalytic degradation of aqueous organic pollutants by UV-irradiated titania. Journal of Catalysis, 2001, 200, 10-20.

Matthews R. Photooxidation of organic impurities in water using thin films of titanium dioxide. Journal of Physical Chemistry, 1987, 91, 3328-3333.

Matthews R. An adsorption water purifier with in situ photocatalytic regeneration. Journal of Catalysis, 1988, 113, 549-555.

Matthews R. Photocatalysis in water purification: Possibilities, problems and prospects. Photocatalytic Purification and Treatment of Water and Air, 1993, 121.

Minero C, Catozzo F, Pelizzetti E. Role of adsorption in photocatalyzed reactions of organic molecules in aqueous TiO_2 suspensions. Langmuir, 1992, 8, 481-486.

Nagaoka S, Hamasaki Y, Ishihara S, Nagata M, Iio K, Nagasawa C, Ihara H. Preparation of carbon/TiO_2 microsphere composites from cellulose/TiO_2 microsphere composites and their evaluation. Journal of Molecular Catalysis A: Chemical, 2002, 177, 255-263.

Ohtani B, Nishimoto S. Effect of surface adsorption of aliphatic alcohols and silver ion on the photocatalytic activity of TiO2 suspended in aqueous solutions. Journal of Physical Chemistry, 1993, 97, 920-926.

Orcel G. The chemistry of silica sol-gel. Ph.D. Dissertation. University of Florida, Gainesville, Fl, 1987.

Peral J, Casado J, Domenech J. Light-induced oxidation of phenol over ZnO powder. Journal of Photochemistry and Photobiology A: Chemistry, 1988, 44, 209-217.

Powers K. The development and characterization of sol gel substrates for chemical and optical applications. Ph.D. Dissertation. University of Florida, Gainesville, FL, 1998.

Serpone N. Brief introductory remarks on heterogeneous photocatalysis. Solar Energy Material and Solar Cells, 1995, 38, 369-379.

Skubiszewska-Zieba J, Charmas B, Leboda R, Staszczuk P, Kowalczyk P, Oleszczuk P. Effect of hydrothermal modification on the porous structure and thermal properties of carbon-silica adsorbents (carbosils). Materials Chemistry and Physics, 2002, 78, 486-494.

Tanaka K, Hisanaga T, Rivera P. Effect of crystal form of TiO_2 on the photocatalytic degradation of pollutants. Photocatalytic purification and treatment of water and air, 1993, 169.

Torimoto T, Ito S, Kuwabata S, Yoneyama H. Effects of adsorbents used as supports for titanium dioxide loading on photocatalytic degradation of propyzamide. Environmental Science and Technology, 1996, 30, 1275-1281.

Torimoto T, Okawa Y, Takeda N, Yoneyama H. Effect of activated carbon content in TiO_2-loaded activated carbon on photodegradation behaviors of dichloromethane. Journal of Photochemistry and Photobiology A: Chemistry, 1997, 103, 153-157.

Turchi C, Ollis D. Mixed reactant photocatalysis: Intermediates and mutual rate inhibition. Journal of Catalysis, 1989, 119, 483-496.

Turchi C, Ollis D. Photocatalytic degradation of organic water contaminant mechanisms involving hydroxyl radical attack. Journal of Catalysis, 1990, 122, 178-192.

Villieras F, Leboda R, Charmas B, Bardot F, Gerard G, Rudzinski W. High resolution argon and nitrogen adsorption assessment of the surface heterogeneity of carbosils. Carbon, 1998, 36, 10, 1501-1510.

Vohra M, Tanaka K. Photocatalytic degradation of aqueous pollutants using silica-modified TiO_2. Water Research, 2003, 37, 3992-3996.

Xu Y, Zheng W, Liu W. Enhanced photocatalystic activity of supported TiO2 dispersing effect of SiO_2. Journal of Photochemistry and Photobiology A: Chemistry, 1999, 122, 57-60.

Yoneyama H, Torimoto T. Titanium dioxide/adsorbent hybrid photocatalysts for photodestruction of organic substances of dilute concentrations. Catalysis Today, 2000, 58, 133-140.

BIOGRAPHICAL SKETCH

Christina Yvette TerMaath was born in Lafayette, Indiana, on January 7, 1977. Her family spent a few years in Lafayette and Panama City, Florida, before relocating to Springfield, Virginia, where Christina graduated from West Springfield High School in 1995. She pursued a Bachelor of Science degree in Chemical Engineering from the Pennsylvania State University with a focus on energy and fuels. Her interest in environmental engineering was realized as she studied the pollution and control of emissions from the use of fossil fuels. Upon graduation in December 1999, Christina began an eight month internship with the US Environmental Protection Agency in Washington, DC, where her interest in environmental engineering grew. After two years at an energy consulting company in Washington, DC, where she learned about hydrogen fuel technologies through her work with the Department of Energy's Hydrogen Program, Christina decided to pursue graduate school in the Environmental Engineering Sciences Department at the University of Florida.